

Contents lists available at ScienceDirect

Earth-Science Reviews

journal homepage: [www.elsevier.com/locate/earscirev](http://www.elsevier.com/locate/earscirev)

# Climate change impacts on groundwater and soil temperatures in cold and temperate regions: Implications, mathematical theory, and emerging simulation tools

Barret L. Kurylyk<sup>a,\*</sup>, Kerry T.B. MacQuarrie<sup>a</sup>, Jeffrey M. McKenzie<sup>b</sup>

<sup>a</sup> Department of Civil Engineering, University of New Brunswick, PO Box 4400, Fredericton, NB E3B 5A3, Canada

<sup>b</sup> Earth and Planetary Sciences Department, McGill University, 3450 University Street, Montreal, QC H3A 0E8, Canada

## ARTICLE INFO

### Article history:

Received 1 June 2013

Accepted 21 June 2014

Available online xxxx

### Keywords:

Climate warming

Thermal regime

Permafrost thawing

Analytical solutions

Numerical modeling

Cryohydrogeology

## ABSTRACT

Climate change is expected to increase regional and global air temperatures and significantly alter precipitation regimes. These projected changes in meteorological conditions will likely influence subsurface thermal regimes. Increases in groundwater and soil temperatures could impact groundwater quality, harm groundwater-sourced ecosystems, and contribute to the geotechnical failure of critical infrastructure. Furthermore, permafrost thaw induced by rising subsurface temperatures will likely alter surface and subsurface hydrology in high altitude and/or latitude regions and exacerbate the rate of anthropogenic climate change by releasing stored carbon into the atmosphere.

This contribution discusses the theory and development of subsurface heat transport equations for cold and temperate regions. Analytical solutions to transient forms of the conduction equation and the conduction–advection equation with and without freezing are detailed. In addition, recently developed groundwater flow and heat transport models that can accommodate freezing and thawing processes are briefly summarized. These models can be applied to simulate climate change-induced permafrost degradation and dormant aquifer activation in cold regions. Several previous reviews have focused on the impact of climate change on subsurface hydraulic regimes and groundwater resources, but this is the first synthesis of studies considering the influence of future climate change on subsurface thermal regimes in cold and temperate regions. The current gaps in this body of knowledge are highlighted, and recommendations are made for improving future studies by linking atmospheric global climate models to subsurface heat transport models that consider heat advection via groundwater flow.

© 2014 Elsevier B.V. All rights reserved.

## Contents

1.	Introduction	0
2.	Subsurface thermal and hydrogeological processes in permafrost regions	0
2.1.	Thermal processes in cold regions	0
2.2.	Hydrogeological processes in cold regions	0
2.3.	Subsurface effects of climate change in cold regions	0
3.	The theory of subsurface heat transport including heat advection via groundwater flow and the latent heat associated with freeze–thaw	0
3.1.	Heat transport modes	0
3.2.	Conduction-only heat transport equation	0
3.3.	Conduction–advection heat transport equation	0
3.4.	Thermal dispersion	0
3.5.	Subsurface thermal properties	0
3.6.	Latent energy effects of freezing and thawing	0
3.7.	Dimensionless numbers for subsurface heat transport	0
4.	Analytical solutions to simplified heat transport equations	0
4.1.	Analytical solutions to the conduction equation subject to surface temperature changes	0
4.2.	Analytical solutions to the conduction–advection equation in a stable climate	0
4.3.	Analytical solutions to the conduction–advection equation subject to long term surface temperature changes	0

\* Corresponding author. Tel.: +1 506 453 4521.

E-mail addresses: [barret.kurylyk@unb.ca](mailto:barret.kurylyk@unb.ca) (B.L. Kurylyk), [ktm@unb.ca](mailto:ktm@unb.ca) (K.T.B. MacQuarrie), [jeffrey.mckenzie@mcgill.ca](mailto:jeffrey.mckenzie@mcgill.ca) (J.M. McKenzie).

4.4.	Analytical solutions for subsurface heat transport with freezing and thawing	0
5.	Numerical models of groundwater flow and heat transport	0
5.1.	Early numerical modeling of groundwater flow and heat transport	0
5.2.	Contemporary groundwater flow and heat transport models	0
5.3.	Groundwater flow and heat transport models that include freeze–thaw	0
6.	Simulated climate change impacts on groundwater flow and heat transport in cold and temperate regions	0
7.	Discussion and conclusions	0
7.1.	The role of advective heat transport in accelerating permafrost thaw	0
7.2.	Emerging datasets for model assessment	0
7.3.	Translating climate model output to subsurface model boundary conditions	0
7.4.	Advancing future research in non-permafrost regions	0
	Acknowledgments	0
	References	0

## 1. Introduction

This review details the current state of knowledge regarding subsurface heat transport processes and the sensitivity of subsurface thermal regimes to climate change. The formal study of terrestrial heat transport was initiated when the theories described in Fourier's (1822) classic treatise on heat conduction were applied by Kelvin (1861) to consider heat transport phenomena within the earth's subsurface. The investigation of the impact of groundwater flow (heat advection) on subsurface thermal regimes began in the twentieth century when Bullard (1939) proposed that heat flow anomalies in boreholes could be induced by fluid flow. Over the past two centuries, engineers and geoscientists have advanced the theory of heat transport in shallow and deep subsurface environments and have applied this theory in agricultural science and engineering (e.g., Balland et al., 2006; Mellander et al., 2007; Kahimba et al., 2009), geotechnical engineering (e.g., Lunardini, 1981; Krzewinski and Tart, 1985; Andersland and Ladanyi, 1994), paleoclimatology/thermal geophysics (e.g., Beltrami et al., 1995; Bodri and Cermak, 2007; Lesperance et al., 2010) and hydrology (e.g., Williams and Smith, 1989; Luo et al., 2003; Woo, 2012).

More recently, groundwater and soil temperature research has primarily focused on subsurface thermal energy storage and extraction (e.g., Molina-Giraldo et al., 2011; Hähnlein et al., 2013; Bridger and Allen, 2014), the utilization of heat as a hydrological tracer (e.g., Anderson, 2005; Hatch et al., 2006; Saar, 2011; Gordon et al., 2012), the ecohydrology of groundwater–surface water interactions (e.g., Alexander et al., 2003; Engeler et al., 2011; Kløve et al., 2011), the subsurface thermal impact of urbanization (e.g., Ferguson and Woodbury, 2007; Taniguchi et al., 2008; Menberg et al., 2013; Zhu et al., 2014), and the thermal influence of future climate change (e.g., Taylor and Stefan, 2009; Lawrence et al., 2012; Kurylyk et al., 2014a).

Increases in groundwater temperatures have been observed due to the rapid climate warming experienced in the past century (Figura et al., 2011; Bloomfield et al., 2013; Menberg et al., 2014), and these trends are expected to intensify in the coming decades (Gunawardhana et al., 2011; Kurylyk et al., 2013). The impact of climate change on groundwater and soil temperatures in cold regions is an emerging concern, as permafrost thaw may cause the release of sequestered carbon (e.g., Solomon et al., 2007; Schaefer et al., 2011; Wissler et al., 2011; Harden et al., 2012; McGuire et al., 2012). Climate change-induced increases in subsurface temperatures could also affect biogeochemical processes and, consequently, groundwater quality (Rike et al., 2008; Green et al., 2011; Sharma et al., 2012). Given that groundwater supplies almost half of the global drinking water demand (van der Gun, 2012), climate change impacts on groundwater temperature and quality are an international concern.

The sensitivity of subsurface thermal regimes to climate change is also important from an ecohydrology perspective. Groundwater

temperature tends to be cooler than surface water temperature in the summer, and warmer in the winter (Hayashi and Rosenberry, 2001). Thus diffuse groundwater discharge can reduce diel and seasonal temperature variability in streams and rivers, and discrete groundwater discharge can create in-stream thermal anomalies that provide cold-water thermal refugia for aquatic species during summer months (Breau et al., 2011; Briggs et al., 2013; Kurylyk et al., 2014a). Hence, rising groundwater temperatures induced by climate change may be potentially deleterious to lotic ecosystems. The uncertainty surrounding the future thermal states of shallow aquifers has been a challenge to surface water temperature analysts attempting to estimate the thermal sensitivity of streams and rivers to climate change and the resultant loss of habitat for cold-water fishes (e.g., Mayer, 2012; Kanno et al., 2014).

Although there is an emerging body of research examining the subsurface thermal impact of climate change, there has not been a comprehensive review of the important implications of subsurface temperature rise or of the analytical and numerical simulation approaches available for conducting these analyses. Several recent reviews (Anderson, 2005; Constantz, 2008; Saar, 2011; Rau et al., 2014) have synthesized the existing literature pertaining to the application of subsurface heat transport theory to trace the direction and magnitude of groundwater flow from measured temperature–depth profiles or streambed temperature–time series. Other recent reviews have summarized the state of knowledge on the effects of climate change on groundwater resources (Green et al., 2011; Kurylyk and MacQuarrie, 2013; Taylor et al., 2013), but these contributions were focused on the subsurface hydrologic impact of climate change rather than the thermal impact. Another recent contribution (Riseborough et al., 2008) reviewed the advances in permafrost modeling made in the past decade and the remaining challenges in modeling subsurface heat transport in cold regions. The scope of the present review is the impact of future climate change on subsurface (i.e., soil and groundwater) temperatures, with a particular focus on cold regions where climate warming is expected to be most severe (Meehl et al., 2007). In particular, the current review considers the physical processes governing subsurface heat transport, the mathematical formulae used to describe these processes, and the application of analytical and numerical solutions to obtain answers to well-posed questions regarding the subsurface thermal effects of future climate change. Thus it builds upon and complements previous reviews that have focused on climate change, subsurface thermal regimes, or cold region heat transport and hydrogeology.

Section 2 describes groundwater flow and heat transport processes in permafrost regions. This topic demonstrates the importance of subsurface heat transport in the context of climate change, particularly for cold regions. Section 3 develops the relevant theory for terrestrial heat transport and is presented in sufficient detail to inform and equip researchers who are new to this field. Section 4 reviews the development and application of several analytical solutions to transient forms of the conduction equation and the conduction–advection equation with and

without the thermal effects of soil thawing considered. These solutions have been compiled for a variety of boundary conditions which are intended to represent surficial climate change. Section 5 describes recent advances in the numerical modeling of groundwater flow and heat transport, particularly for hydrogeological systems that experience pore water freeze–thaw, and briefly lists several emerging models. Section 6 reviews recent studies that have applied numerical models to simulate the interrelationships between climate change, groundwater flow, and subsurface temperature evolution. Section 7 concludes by providing several recommendations for improving future studies investigating the subsurface thermal response to climate change.

## 2. Subsurface thermal and hydrogeological processes in permafrost regions

### 2.1. Thermal processes in cold regions

High latitude or high altitude regions can contain permafrost, which has been defined as ground that remains below 0 °C for two or more consecutive years (Dobinski, 2011). Permafrost is a dominant morphological feature that extends across almost a quarter of the exposed terrestrial surface of the northern hemisphere (Bonan, 2008). The distribution of permafrost can be affected by many factors including air temperature, vegetation, land-surface slope, and aspect (e.g., Shur and Jorgenson, 2007; Jorgenson et al., 2010). Permafrost regions are typically classified as continuous permafrost (often at higher latitudes) and discontinuous permafrost (often at lower latitudes) based on spatial cover, and these two permafrost zones are typically separated at a mean annual ground temperature of −5 °C (Brown, 1970). Others (e.g., Williams, 1970) include another zone at lower latitudes, known as sporadic permafrost, which is separated from discontinuous permafrost at a temperature of −1 °C. Finally, others (e.g. Heginbottom et al., 1993) have proposed still another classification, known as isolated permafrost, which describes regions where permafrost underlies less than 10% of the land surface area.

Permafrost is overlain by an active layer that freezes and thaws on an annual basis (Williams and Smith, 1989; Woo, 2012; Quinton and Baltzer, 2013). The bottom depth of permafrost (permafrost base) is limited by the geothermal gradient and mean annual surface temperature, and the upper limit of permafrost (permafrost table) is controlled by energy fluxes across the ground surface (Fig. 1). The difference in depth between the permafrost table and the permafrost base is the permafrost thickness. The thickest permafrost (~1.5 km) has been recorded in northeastern Siberia (Brown, 1970).

Shallow subsurface thermal regimes are primarily driven by heat transfer across the ground surface. Seasonal variations in the ground surface temperature are propagated through the shallow subsurface via conductive and advective heat transfer; however, the amplitude of the seasonal temperature variation is exponentially damped with depth (Lesperance et al., 2010). The seasonal penetration depth is the depth at which the seasonal surface temperature variations are almost (e.g., 99%) fully damped due to the heat capacity of the soil and pore water or ice (Bonan, 2008). In a stable climate and in the absence of groundwater flow or significant thermal property heterogeneities, the temperature–depth profile below the seasonal penetration depth is characterized by the geothermal gradient. These thermal processes and the associated terminology are indicated in Fig. 1, which assumes a stable climate and negligible groundwater flow. The effect of groundwater flow on subsurface thermal regimes will be discussed in detail in Sections 2.2 and 3.

### 2.2. Hydrogeological processes in cold regions

Groundwater flow in permafrost regions is often assumed to be negligible due to the hydraulic impedance caused by pore ice (French, 2007). However, groundwater may remain unfrozen at temperatures below 0 °C due to the freezing point depression caused by solute concentration, positive pressure, and capillary and sorptive forces (Koopmans and Miller, 1966; Miller, 1980; Kurylyk and Watanabe, 2013). Thus, because permafrost is a temperature-based definition, rather than a reference to the physical state of the pore fluid, permafrost zones close to 0 °C can contain unfrozen pore water and provide

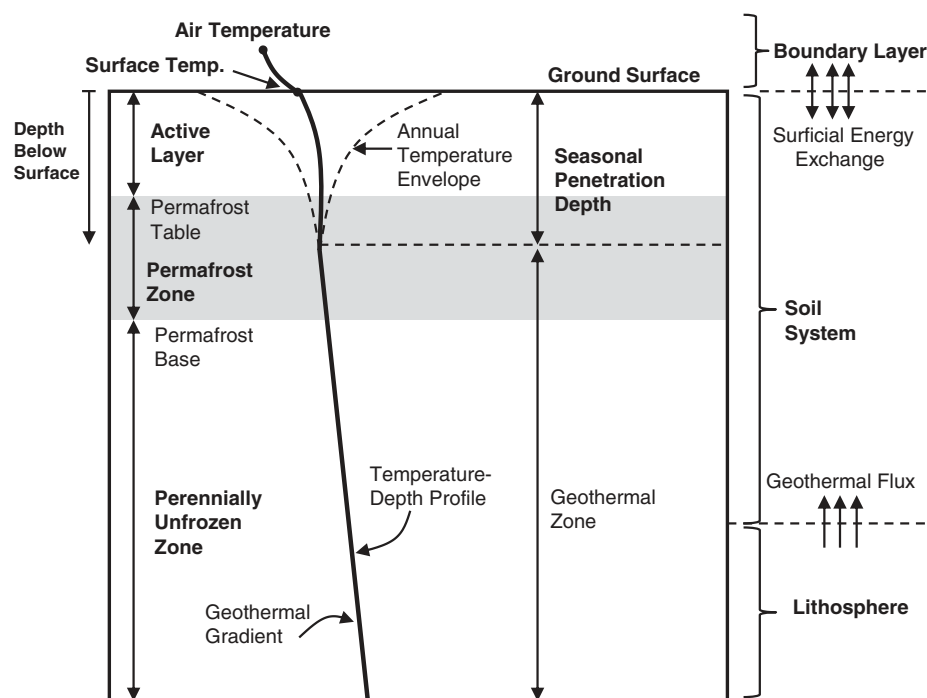


**Fig. 1.** A typical subsurface temperature–depth profile for a permafrost region. The active layer and permafrost zone are shown to the left of the temperature–depth profile. The seasonally varying temperature zone and the geothermal zone are indicated to the right of the temperature–depth profile. The energy exchanges between the soil and the lithosphere and boundary layer are shown to the far right (modified from Williams and Smith, 1989; Lunardini, 1985; Dobinski, 2011).

suitable media for active groundwater systems. The study of groundwater in permafrost, referred to as cryohydrogeology, has typically received very little attention in hydrological literature (Woo et al., 2008). However, there has recently been a renewed interest in cryohydrogeology due to the potential interactions between climate change, permafrost degradation, and groundwater flow (e.g., Callegary et al., 2013; Cheng and Jin, 2013; Frampton et al., 2013; McKenzie and Voss, 2013; Wellman et al., 2013).

Even in regions of continuous permafrost, where mean annual air temperature is significantly below zero, three zones of groundwater flow can exist. (1) Groundwater in the active layer (Figs. 1 and 2) is known as supra-permafrost groundwater. Supra-permafrost aquifers generally exhibit seasonally active (summer) and dormant (winter) cycles (Woo, 1986; Freitag and McFadden, 1997; Woo, 2012). The permafrost typically acts as a barrier layer (or 'time dependent aquitard', Cheng and Jin, 2013) between the groundwater zones above and below the permafrost (Williams, 1970; Freitag and McFadden, 1997; Haldorsen et al., 2010). (2) Unfrozen zones within the permafrost layer can provide conduits for in-permafrost groundwater flow (Fig. 2). Cheng and Jin (2013) further divide in-permafrost groundwater into (2a) en-permafrost groundwater, which is completely surrounded by permafrost; (2b) intra-permafrost groundwater, which is bounded by permafrost at the top and bottom; and (2c) talik channel groundwater, which is laterally bounded by permafrost. Taliks are unfrozen zones that are often formed by heat flowing from surface water bodies or heated buildings. They can be found at temperatures below 0 °C if the dissolved mineral content of the pore water is high (French, 2007). Vertical taliks that extend through the entire permafrost zone are known as open taliks or through-going taliks. (3) The third zone of groundwater is sub-permafrost groundwater (Fig. 2), which exists due to the geothermal gradient and which can provide a medium for regional groundwater flow. For example, Kane et al. (2013) postulated that the source of groundwater discharge from taliks in a continuous permafrost zone in northeast Alaska was recharged water from the south side of a

mountain range that was transmitted to the taliks via a sub-permafrost aquifer.

### 2.3. Subsurface effects of climate change in cold regions

Climate change is projected to be most severe at high latitudes (Meehl et al., 2007), and observed hydrologic and ecological changes to Arctic and subarctic regions due to climate warming have been well summarized (Rouse et al., 1997; Serreze et al., 2000; Jorgenson et al., 2001; Hinzman et al., 2005; Schindler and Smol, 2006). These changes include decreasing sea ice, permafrost warming or degradation, increased carbon dioxide release from soils, decreased glacier ice mass, and shifting biological indicators. For example, increases in soil temperatures have been directly observed from long-term measurements or inferred from borehole temperature profiles in high latitude or altitude regions of North America (e.g., Romanovsky and Osterkamp, 1997; Smith et al., 2010; Qian et al., 2011; Quinton et al., 2011), Asia (e.g., Zhang et al., 2001; Yang et al., 2010; Wu et al., 2012), and Europe (e.g., Mauro, 2004; Harris et al., 2009; Eitzelmüller et al., 2011; Hipp et al., 2012). As the climate warms, an imbalance arises between the rate of permafrost aggradation and degradation, and thus the thickness and aerial extent of permafrost is reduced (Quinton and Baltzer, 2013). In China, permafrost area has decreased almost 20% in the past 30 years (Cheng and Jin, 2013). Romanovsky et al. (2010) provided a synthesis of the present thermal state of permafrost in the polar Northern Hemisphere and stated that significant permafrost warming (up to 2 °C) has occurred for the past two to three decades. The rate of permafrost degradation is expected to accelerate in the coming decades due to intensive global warming. For instance, Schaefer et al. (2011) used output from three global climate models (GCMs) to simulate a 29–59% reduction in global permafrost area by 2200. Lawrence et al. (2012) used the land surface component of a GCM to simulate a range of reductions (33–72%) in global near-surface permafrost by 2100 for two climate warming projections.

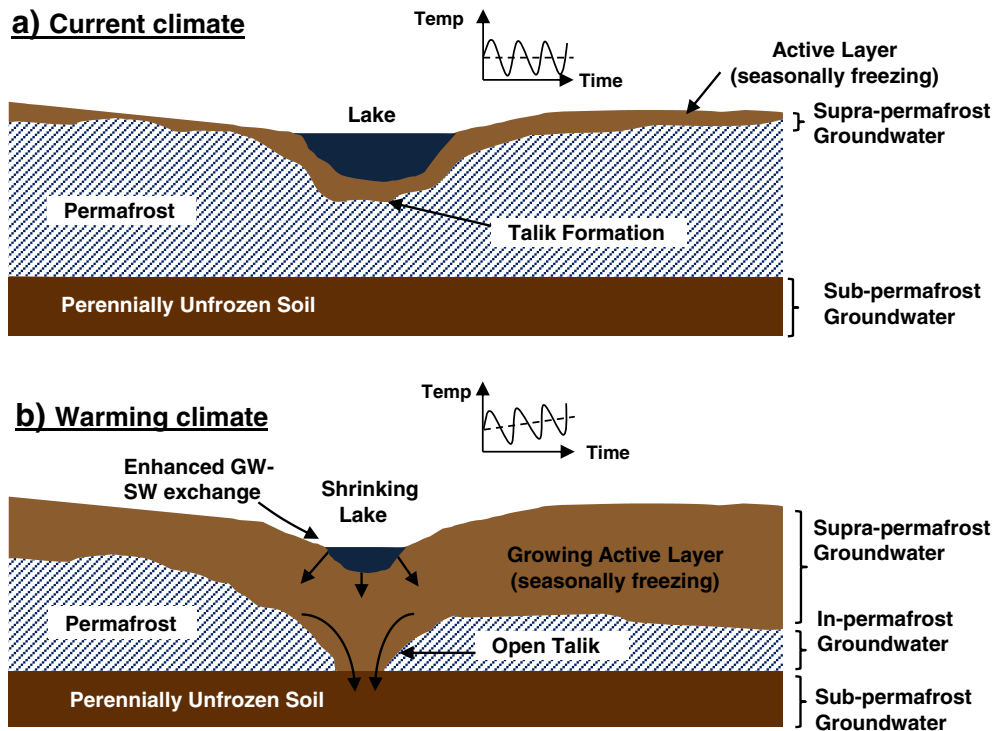


Fig. 2. Potential subsurface thermal and hydrologic effects of rising air and ground surface temperature in cold regions. Heat conduction from rising surface temperatures thaws the underlying permafrost, and heat advection from draining surface water bodies accelerates the rate of thaw (modified from Williams, 1970; Freitag and McFadden, 1997). New open taliks may facilitate groundwater-surface water (GW-SW) exchange.

There is considerable concern that permafrost thaw could act as a positive feedback mechanism to future climate change by releasing carbon and methane stored in northern soils (e.g., Kettridge and Baird, 2008; Tarnocai et al., 2009; Harden et al., 2012). Currently, Arctic and boreal soils contain about 40% of the global terrestrial carbon, and this undergoes very little decomposition (Gouttevin et al., 2012). Thus, in the recent past, soil in northern muskeg and peatlands has provided storage for global carbon (Marshall, 2012). However, climate change can accelerate the rate of decomposition in these organic soils and transform northern soils from a global carbon sink to a global carbon source (Oechel et al., 1993; Romanovsky and Osterkamp, 1997). Additionally, increased groundwater discharge from thawing permafrost aquifers with organic soils could lead to increased dissolved organic carbon contents in rivers. This will in turn increase respiration rates and the concentration of atmospheric CO<sub>2</sub> (Lyon et al., 2009). Thus, understanding and characterizing permafrost degradation are integral components of the broader scientific study of the role of climate change in altering Arctic hydrology, ecology, and biochemistry (Lawrence et al., 2012).

As air and surface temperatures rise, the surficial temperature signal is propagated through the subsurface, and the shallow permafrost will begin to warm. The thickness of the active layer will increase over time, which in turn reduces the permafrost thickness (Pang et al., 2012; Streletskiy et al., 2012). Previously closed taliks may expand and become open taliks that extend through the entire permafrost thickness, thereby facilitating hydraulic interactions between supra-permafrost and sub-permafrost aquifers (Fig. 2). Also, the number of lakes with mean annual bed temperatures above 0 °C is expected to increase due to rising air temperatures, and this will likely produce a larger number of sub-lake taliks (Matell et al., 2013). As Fig. 2c indicates, these taliks can provide conduits to rapidly drain Arctic lakes (Smith et al., 2005) and accelerate permafrost degradation due to heat transfer associated with moving groundwater (Bense et al., 2012; McKenzie and Voss, 2013).

As the pore ice begins to melt, the permeability of the soil increases, and hydraulic exchanges between surface water bodies and supra-permafrost groundwater are enhanced (Fig. 2). Thus aquifer activation arising from permafrost degradation may increase baseflow to rivers and lakes and reduce seasonal variability in river flows (Michel and van Everdingen, 2006). Such changes have been observed or simulated in numerous studies (Smith et al., 2007; Walvoord and Striegl, 2007; Lyon et al., 2009; St. Jacques and Sauchyn, 2009; Walvoord et al., 2012; Connon et al., 2014). Winter groundwater discharge can warm rivers and lakes in cold regions (Utting et al., 2012), and thus increased baseflow arising from permafrost thaw may reduce the thickness and duration of winter ice cover (Jones et al., 2013). This is a concern for northern communities that utilize ice roads for transportation. The quality of groundwater will likely also be affected by degrading permafrost, because the presence of permafrost affects the residence time in aquifers and thus the time available for biogeochemical reactions between the pore water and soil particles (Williams, 1970).

The degradation of permafrost also decreases the strength properties of soil. For example, the stability of slopes in permafrost regions is often maintained by ice-filled joints. These joints become unstable as the temperature warms, and mass-wasting events can occur (Davies et al., 2001; Gruber and Haerberli, 2007; Zhang and Wu, 2012). This can occur even if the ice does not fully thaw, as the shear strength of ice decreases as it approaches the melting temperature (Harris et al., 2009). The link between climate warming and slope instability has been demonstrated by numerous researchers. For example, Fischer et al. (2006) studied slope instabilities and detachment zones in the Italian Alps and concluded that recent permafrost degradation was the primary culprit. Geotechnical failure induced by climate warming in permafrost regions may also arise due to a reduction in the bearing capacity of warming permafrost (Vyalov et al., 1993; Anisimov and Reneva, 2006). Weakened soil properties due to permafrost

degradation can also alter ecosystems. For example, previously forested regions are being converted to bogs and fens due to a removal of their soil foundation and other altered physical and thermal conditions (Jorgenson et al., 2001; Jiang et al., 2012a).

Another result of permafrost degradation is land subsidence. When ice-rich permafrost thaws, the ground surface may subside and form irregular surface features known as thermokarst that can be deleterious to ecosystems (Serreze et al., 2000). Thermokarst depressions may preferentially form taliks and drain surface water bodies (Yoshikawa and Hinzman, 2003; Callegary et al., 2013). Permafrost thaw-induced subsidence can also harm infrastructure such as roads, pipelines, and buildings by causing differential settlement (Jin et al., 2006; de Grandpre et al., 2012). Further details on the geotechnical properties of soils and their sensitivity to climate are given by Andersland and Anderson (1978), Williams and Smith (1989), Andersland and Ladanyi (1994), and Freitag and McFadden (1997).

In summary, subsurface thermal environments in colder regions are highly susceptible to climate change due to the magnitude of the changes projected for these regions and the particular sensitivity of cryosols to surficial thermal perturbations. In permafrost regions, changes to soil temperatures may result in failed infrastructure, changing surface and subsurface hydrologic conditions, and altered ecosystems.

### 3. The theory of subsurface heat transport including heat advection via groundwater flow and the latent heat associated with freeze–thaw

#### 3.1. Heat transport modes

There are three modes of heat transport in the shallow subsurface: conduction, convection, and radiation. Conduction is a diffusive mode of heat transport that occurs when colliding molecules exchange energy by atomic vibrations (Bear, 1972; Lunardini, 1981). In liquid water, conductive heat transport is also caused by the formation and breaking of hydrogen bonds (Farouki, 1981b). Conduction is a thermally homogenizing force that induces heat transfer from high temperature regions to low temperature regions until thermal equilibrium is achieved.

Heat conduction has been shown to be directly proportional to the temperature gradient according to Fourier's law (Özıık, 1980; Lunardini, 1981):

$$\underline{q}_{cond} = -\underline{\lambda}\nabla(T) \quad (1)$$

where  $\underline{q}_{cond}$  is the vector of conductive heat flux ( $W\ m^{-2}$ ),  $\underline{\lambda}$  is the thermal conductivity tensor of the medium ( $W\ m^{-1}\ ^\circ C^{-1}$ ), and  $\nabla(T)$  is the gradient of the temperature field ( $^\circ C\ m^{-1}$ ). All symbols are also defined in Table 1. If the domain is homogeneous and isotropic with respect to thermal conductivity, the tensor simplifies to a single value  $\lambda$ . Note that throughout this review, we employ Celsius as the temperature scale, as it is a more convenient in the discussions related to permafrost and soil thaw given that soil thawing occurs near 0 °C.

Convection is the only mode of heat transport associated with the movement of mass (Bear, 1972; Lunardini, 1981). Within the subsurface, convective heat transport is usually induced by the movement of pore water, although convective transport due to water vapor migration can occur within the unsaturated zone. 'Free' convection arises from density driven flow caused by temperature gradients, and 'forced' convection occurs due to groundwater flow induced by a hydraulic gradient (Domenico and Schwartz, 1990). The term advection is commonly used in hydrogeology to refer to forced convection. In the absence of significant vapor flow, advective heat flux  $\underline{q}_{adv}$  ( $W\ m^{-2}$ ) is a function of the groundwater velocity vector  $\underline{v}$  ( $m\ s^{-1}$ ), the mobile saturation of the liquid water phase  $S_{wm}$  (volume of mobile water/porosity), the porosity  $\epsilon$ , the liquid water density  $\rho_w$  ( $kg\ m^{-3}$ ), the temperature  $T$

**Table 1**  
List of symbols and definitions used in this paper.

Symbol	Definition	Symbol	Definition
$\alpha$	Thermal diffusivity ( $\lambda/\rho c$ )	$\mu_w$	Dynamic viscosity of water
$\alpha_A$	Apparent thermal diffusivity	$P_e$	Dimensionless Peclet number
$\alpha_u$	Thermal diffusivity of unfrozen media	$P_e^*$	Basin scale Peclet number
$\alpha_f$	Thermal diffusivity of frozen media	$\psi$	Rate of surficial temperature rise
$B$	Vertical basin dimension	$q_z$	Darcy velocity in vertical direction
$C_a$	Apparent heat capacity due to latent heat	$q_{adv}$	Advective heat flux
$c$	Specific heat of soil–water matrix	$q_{cond}$	Conductive heat flux
$c_a$	Specific heat of air	$R$	Thermal plume retardation factor
$c_i$	Specific heat of ice	$R_{th}$	Thaw retardation factor
$c_s$	Specific heat of solid grain particles	$\rho$	Bulk density of soil–water medium
$c_w$	Specific heat of water	$\rho_a$	Density of air
$d$	Thermal dispersivity	$\rho_i$	Density of ice
$\nabla$	Del operator (gradient)	$\rho_s$	Density of solid grain particles
$\varepsilon$	Porosity	$\rho_w$	Density of water
erf	Error function	$S_i$	Saturation of ice
erfc	Complementary error function	$S_{ip}$	Ice sat. that undergoes phase change
$g$	Acceleration due to gravity	$S_w$	Saturation of water
$G$	Geothermal gradient	$S_{wm}$	Mobile water saturation
$H$	Horizontal basin dimension	$S_T$	Dimensionless Stefan number
$I_{th}$	Surface thaw index	$T$	Temperature
$k$	Permeability of aquifer	$t$	time
$\kappa$	Duration of temp. increase (Eq. 20c)	$T_0$	Initial surface temperature
$\lambda$	Thermal conductivity of soil–water matrix	$T_f$	Freezing temperature
$\lambda_A$	Apparent thermal cond. including dispersion	$T_i$	Initial temperature of soil
$\lambda_a$	Thermal conductivity of air	$T_j$	Final temperature of soil
$\lambda_f$	Thermal conductivity of frozen media	$T_s$	Surface temperature
$\lambda_i$	Thermal conductivity of ice	$T_s(t)$	Surface temperature function
$\lambda_s$	Thermal conductivity of solid grain particles	$\Delta T$	Step change in surface temperature
$\lambda_u$	Thermal conductivity of unfrozen media	$\theta_i$	Volumetric content of ice = $\varepsilon S_i$
$\lambda_w$	Thermal conductivity of water	$U$	= $q_z c_w \rho_w / (c\rho)$ (Eq. (18))
$\lambda$	Thermal conductivity of bulk media	$v$	Groundwater velocity
$L_f$	Latent heat of fusion for water	$X(t)$	Depth of freeze thaw interface
$L^*$	Characteristic length	$z$	Depth below ground surface
$m$	Coefficient of proportionality for thawing soils	$\Delta z$	Water table relief

(°C), and the liquid water specific heat  $c_w$  ( $\text{J kg}^{-1} \text{ }^\circ\text{C}^{-1}$ ) (Domenico and Schwartz, 1990; Saar, 2011):

$$q_{adv} = v S_{wm} \varepsilon c_w \rho_w T. \tag{2}$$

The magnitude of the advective flux calculated with Eq. (2) is dependent on the temperature scale utilized (e.g., Kelvin or Celsius). Eq. (2) can be expressed with fewer terms by replacing the product of  $v$ ,  $S_{wm}$ , and  $\varepsilon$  with the Darcy velocity.

Any mass at a temperature above absolute zero emits radiation at a radiant flux density proportional to the fourth power of its absolute temperature according to the Stefan–Boltzmann law (Bonan, 2008). Although this radiant energy can be propagated through solids, liquids, or gasses, it is typically rapidly absorbed in a solid or liquid (Domenico and Schwartz, 1990). Radiation can be significant in groundwater flow and heat transport studies, but only at high temperatures (e.g., 600 °C, Ingebritsen et al., 2006). As such, radiation is typically ignored in shallow subsurface heat transport studies.

In a conduction-dominated system, the subsurface thermal regime is primarily controlled by a combination of the land surface temperature variations and heat flow from the interior of the earth (Gold and Lachenbruch, 1973). However, groundwater flow induces advective heat transport, which can significantly perturb a conduction-dominated thermal regime (Domenico and Palciauskas, 1973). Similarly, temperature gradients can actuate density-driven groundwater flow. As a result, groundwater flow and heat transport processes are interdependent and are typically considered as coupled processes in studies of subsurface water flow and energy transport.

### 3.2. Conduction-only heat transport equation

If conduction is assumed to be the dominant heat transport mechanism, and freezing and thawing processes are ignored, the governing partial differential equation for subsurface heat transport is the classic

heat diffusion equation (Carslaw and Jaeger, 1959; Özıık, 1980). This states that the divergence of the conductive flux through a control volume can be related to the temporal rate of the change of heat storage within that volume (Lunardini, 1985):

$$\nabla \cdot (\bar{\lambda} \nabla T) = \frac{\partial c\rho T}{\partial t} \tag{3}$$

where  $t$  is time (s),  $c$  is the specific heat of the medium ( $\text{J kg}^{-1} \text{ }^\circ\text{C}^{-1}$ ), and  $\rho$  is the bulk density of the medium ( $\text{kg m}^{-3}$ ). Often the thermal conductivity is assumed to be homogeneous and isotropic, and conduction is assumed to be primarily vertical within the subsurface. Also, the heat capacity is considered to be temporally invariant. For this case, the transient heat conduction equation simplifies further:

$$\lambda \frac{\partial^2 T}{\partial z^2} = c\rho \frac{\partial T}{\partial t} \tag{4}$$

where  $z$  is the vertical distance from a datum and, in the context of this paper, usually precisely means the depth below the ground surface (m).

### 3.3. Conduction–advection heat transport equation

Advection and free convection can be important components of the total subsurface heat transfer in regions of significant groundwater flow or vapor migration due to gradients in hydraulic potential or temperature (Smith and Chapman, 1983; Woodbury and Smith, 1985; de Vries, 1987; Kane et al., 2001). Suzuki (1960) proposed a one-dimensional transient heat transfer equation that considers the influences of both advective and conductive heat fluxes:

$$\lambda \frac{\partial^2 T}{\partial z^2} - q_z c_w \rho_w \frac{\partial T}{\partial z} = c\rho \frac{\partial T}{\partial t} \tag{5}$$

where  $q_z$  is the vertical Darcy flux ( $v \cdot \varepsilon \cdot S_{wm}$ ,  $m \ s^{-1}$ ). The first term on the left side of Eq. (5) represents the divergence of the conductive flux, and the second term represents the divergence of the advective flux. The right side of the equation represents the rate of thermal energy change. There are many assumptions associated with this governing equation including one-dimensional heat transport and groundwater flow, homogeneous and isotropic thermal conductivity, constant pore water phase, spatially and temporally constant groundwater velocity, and isothermal conditions between the water and soil particles. In this development, and in many formulations for numerical models of groundwater flow and heat transport, it has been assumed that significant convective heat transfer does not occur in the vapor phase. However, several authors have suggested or demonstrated that vapor phase convective heat transport and/or the latent heat of vaporization can significantly alter the thermal regime of the shallow unsaturated zone (e.g., Kane et al., 2001; Saito et al., 2006). Other derivations and forms of the subsurface conduction–advection equation are given by Bear (1972), Lunardini (1981), and Domenico and Schwartz (1990). The form given in Eq. (5) is the governing equation for the ‘conduction–advection’ analytical solutions presented in Section 4.

The form of Suzuki’s (1960) equation is very similar to the classic one-dimensional solute advection–dispersion equation (Fetter, 1993), where heat conduction is analogous to solute diffusion/dispersion, heat advection is analogous to solute advection, and heat capacity is analogous to solute storage. Because of the mathematical and physical similarities between heat transport and solute transport, many conceptualize the migration of heat as a thermal ‘plume’ (Markle and Schincariol, 2007; Bridger and Allen, 2010). The thermal plume will not migrate at the Darcy velocity due to differences between the matrix volumetric heat capacity and the volumetric heat capacity of the mobile groundwater (Luce et al., 2013). A portion of the heat energy in the migrating plume is transferred to the soil particles, which is analogous to sorption of migrating contaminants. The dimensionless retardation factor  $R$  is the ratio of the average linear groundwater velocity to the thermal plume velocity. If conductive heat transfer is ignored, the retardation factor can be calculated as the ratio of the effective heat capacity of the medium to the heat capacity of the fluid times its volumetric proportion (Markle and Schincariol, 2007):

$$R = \frac{c_p}{S_{wm} \varepsilon C_w \rho_w} \quad (6)$$

### 3.4. Thermal dispersion

Several authors have noted that groundwater velocity variations at the micro and macro-scale may lead to thermal dispersion (Sauty et al., 1982; Ferguson, 2007; Molina-Giraldo et al., 2011). Although the underlying mechanisms for thermal conduction and thermal dispersion are very different, the resultant impacts (i.e., thermal plume spreading) are similar. Dispersion can be treated by adding the influence of the hydrodynamic dispersivity tensor to the thermal conductivity tensor to form an apparent thermal conductivity tensor  $\underline{\underline{\lambda}}_A$  (Sauty et al., 1982):

$$\underline{\underline{\lambda}}_A = \underline{\underline{\lambda}} + \underline{\underline{d}} c_w \rho_w |\bar{v}| \quad (7)$$

Alternatively, the thermal dispersivity term can be combined with the thermal diffusivity (thermal conductivity/heat capacity) term. This is analogous to combining the mechanical dispersion and molecular diffusion terms when modeling solute transport (Bear, 1972; Fetter, 1993):

$$\underline{\underline{\alpha}}_A = \underline{\underline{\alpha}} + \underline{\underline{d}} \frac{c_w \rho_w}{c_p} |\bar{v}| \quad (8)$$

where  $\underline{\underline{\alpha}}$  is the thermal diffusivity tensor of the medium ( $m^2 \ s^{-1}$ ) and  $\underline{\underline{\alpha}}_A$  is the apparent thermal diffusivity tensor ( $m^2 \ s^{-1}$ ) due to the combined effects of heat diffusion and dispersion.

As noted by Anderson (2005) and Rau et al. (2014), there is still disagreement on the relative importance of thermal dispersion. In contrast to solute transfer, heat transfer occurs through the solid phase, and this limits the effects of tortuosity and dispersion in heat transport relative to solute transport (Bear, 1972). Also, since thermal diffusivity can be two orders of magnitude larger than molecular diffusion, the relative importance of dispersion in heat transport studies is reduced compared to solute transport studies (Bear, 1972). As a result, the effects of thermal dispersion are often ignored in hydrogeological studies; however, research in this field is ongoing (e.g., Rau et al., 2012; Bons et al., 2013).

### 3.5. Subsurface thermal properties

The thermal properties of a representative elementary volume within the subsurface depend on its composition. This dependence arises from the differences in the thermal conductivities and heat capacities of water, air, ice, and soil mineral constituents (see Table 2 for typical values). Because liquid water has a thermal conductivity about 20 times that of air and a heat capacity about 3500 times that of air (Farouki, 1981b), the thermal properties of a soil are strongly dependent on its porosity and degree of saturation. Furthermore, ice has a thermal conductivity approximately four times that of water and a thermal capacity approximately half that of water (Oke, 1978), thus the thermal properties of soil are also dependent on the phase (temperature) of the pore water. As temperature varies, these relationships become more complex.

The mineral composition of a soil can also impact both its thermal conductivity and heat capacity (Oke, 1978). In particular, quartz has a much higher thermal conductivity than other mineral components (Domenico and Schwartz, 1990). The thermal conductivity of a soil is also a function of its density, structure, grain size, and grain contact (Farouki, 1981b). Due to its simultaneous dependence on thermal conductivity and heat capacity, the relationship between thermal diffusivity and liquid moisture content, ice content and mineral composition can be quite complex (Oke, 1978).

Various methods to physically measure the thermal properties of soils have been developed (e.g., Farouki, 1981a, 1981b; Andersland and Ladanyi, 1994; Usowicz, 1995; Hinkel, 1997; Overduin et al., 2006), but for the purpose of mathematical modeling, thermal properties are typically computed from the weighted mean of the volumetric contents of the soil particles, air, water, and ice. Because thermal conductivity is a directional tensor, the bulk thermal conductivity is dependent on the orientation of the medium constituents. This is analogous to computing the equivalent electrical resistance of electrical resistors wired in series or parallel (Bear, 1972; Lunardini, 1981). If the medium constituents can be conceptualized as parallel thermal resistors, the bulk thermal conductivity of the medium ( $\lambda$ ) can be taken as the volumetrically weighted arithmetic mean of the constituent thermal conductivities:

$$\lambda = (1-\varepsilon)\lambda_s + \varepsilon(1-S_w-S_i)\lambda_a + \varepsilon S_w \lambda_w + \varepsilon S_i \lambda_i \quad (9)$$

where  $\lambda_s$ ,  $\lambda_a$ ,  $\lambda_w$ , and  $\lambda_i$  are the thermal conductivities for the soil particles, air, water, and ice respectively ( $W \ m^{-1} \ ^\circ C^{-1}$ ),  $\varepsilon$  is the porosity, and  $S_w$  and  $S_i$  are the water and ice saturations, respectively. A minor variant of the weighted arithmetic mean, the deVries (1963) method, is often employed, which includes additional weighting factors that are obtained from shape functions related to the porosity. If the orientation of the medium constituents would be better represented as thermal resistors in series, a more appropriate effective thermal conductivity could be obtained using the volumetrically weighted harmonic mean. The harmonic mean is lower than the arithmetic mean, therefore often an

**Table 2**  
Thermal properties of common subsurface materials.<sup>a</sup>

Material	Comments	Thermal conductivity	Mean density	Specific heat	Heat capacity
		(W m <sup>-1</sup> °C <sup>-1</sup> )	(kg m <sup>-3</sup> )	(J kg <sup>-1</sup> °C <sup>-1</sup> )	(MJ m <sup>-3</sup> °C <sup>-1</sup> )
Soil grains	Sand/gravel	4.1	2640	835	2.22
Air	10 °C, still	0.025	1.20	1010	0.0012
Ice	0 °C, pure	2.24	920	2100	1.93
Water	4 °C, still	0.57	1000	4180	4.18
Soil (sand)	S <sub>w</sub> = 1, ε = 0.4	2.2	2000	1480	2.96
Soil (peat)	S <sub>w</sub> = 1, ε = 0.8	0.50	1100	3650	4.02

<sup>a</sup> Values compiled from Oke (1978), Markle and Schincariol (2007), and Bonan (2008).

intermediate value, the weighted geometric mean, is applied to estimate the bulk thermal conductivity (Lunardini, 1981):

$$\lambda = \lambda_s^{1-\varepsilon} \lambda_a^{\varepsilon(1-S_w-S_i)} \lambda_w^{\varepsilon S_w} \lambda_i^{\varepsilon S_i} \quad (10)$$

In the case of multi-dimensional heat flow in assumed isotropic medium, the weighted geometric mean is preferred rather than the harmonic or arithmetic means given that heat fluxes in two orthogonal directions cannot both be either parallel or perpendicular to the matrix structure.

Because it is not dependent on the constituent orientation, the bulk heat capacity of a composite medium is typically taken as the volumetrically weighted arithmetic mean of the constituent heat capacities (e.g., Lunardini, 1981; Lapham, 1989; Hansson et al., 2004):

$$c\rho = (1-\varepsilon)c_s\rho_s + \varepsilon(1-S_w-S_i)c_a\rho_a + \varepsilon S_w c_w \rho_w + \varepsilon S_i c_i \rho_i \quad (11)$$

where c<sub>s</sub>, c<sub>a</sub>, c<sub>w</sub>, and c<sub>i</sub> are the mass specific heats of the soil particles, air, water, and ice respectively (J kg<sup>-1</sup> °C<sup>-1</sup>), and ρ<sub>s</sub>, ρ<sub>a</sub>, ρ<sub>w</sub>, and ρ<sub>i</sub> are the densities of the soil particles, air, water, and ice respectively (kg m<sup>-3</sup>). The product of the mass specific heat and the density yields the volumetric heat capacity.

In summary, in addition to being dependent on the mineral composition, soil thermal properties are a function of the liquid, ice, and air saturations, which in turn are dependent on pressure and temperature.

This creates another interdependent relationship between groundwater flow and heat transport. Fig. 3 illustrates the dependence of the bulk thermal conductivity and heat capacity on the liquid and ice saturations of the soil. Thermal conductivity and specific heat values for air, water, ice, and soil particles are compiled in several resources (e.g., Oke, 1978; Farouki, 1981b; Domenico and Schwartz, 1990; Markle et al., 2006; Bonan, 2008).

### 3.6. Latent energy effects of freezing and thawing

In ephemerally freezing soils, the rate of decreasing soil temperature is impeded during initial freezing due to the latent heat released by the freezing of pore water (Woo, 2012). Similarly soil warming and thawing in the late winter or early spring are retarded due to the latent heat required to melt the frozen pore water. Thus, the latent heat of fusion released or absorbed during pore water phase change increases the thermal inertia of the subsurface, and at temperatures close to the freezing point, this latent heat can dominate conductive heat transport (Kay et al., 1981; Williams and Smith, 1989).

The thermal effects of pore water phase change can be conceptualized as an increase in the apparent heat capacity of the soil over the temperature range that freezing occurs. This apparent increase in heat capacity can be accommodated within the governing heat transport equations with a transient source/sink term (depending on the direction of temperature change) equal to the latent heat of fusion of water

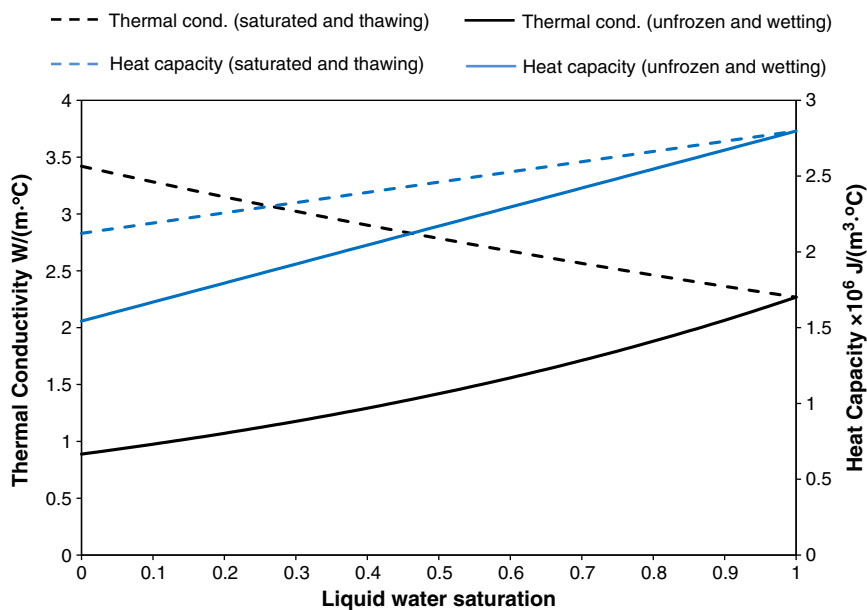


**Fig. 3.** The dependence of a porous medium's thermal conductivity and heat capacity on the liquid water saturation. The thermal conductivity values were calculated using the weighted geometric mean (Eq. (10)), and the heat capacity values were calculated using the weighted arithmetic mean (Eq. (11)). The suggested values for the thermal conductivity and heat capacity of air, water, ice, and soil particles (sand/gravel) given in Table 2 were used for these calculations (porosity = 0.3). The two dashed series represent a fully saturated soil that is thawing. Thus, the ice phase is transitioning to the liquid water phase. The two solid series represent a dry unfrozen soil that is being saturated; thus the air phase is being replaced by the liquid water phase.



$L_f$  (334,000 J kg<sup>-1</sup>) multiplied by the density of ice and the temporal derivative of the volumetric fraction (saturation times porosity) of ice  $\theta_i$  (Kay et al., 1981; Hansson et al., 2004):

$$\text{Source/Sink Term} = -L_f \rho_i \frac{\partial \theta_i}{\partial t} = -L_f \rho_i \frac{\partial \theta_i}{\partial T} \frac{\partial T}{\partial t}. \quad (12)$$

If Eq. (12) is combined with the thermal storage term (right hand side of Eqs. (4) or (5)), an expression for the apparent heat capacity,  $C_a$ , can be formulated (Goodrich, 1982a; Williams and Smith, 1989; Lunardini, 1991; Hansson et al., 2004):

$$c\rho \frac{\partial T}{\partial t} - L_f \rho_i \frac{\partial \theta_i}{\partial T} \frac{\partial T}{\partial t} = \left( c\rho - L_f \rho_i \frac{\partial \theta_i}{\partial T} \right) \frac{\partial T}{\partial t} \quad (13)$$

$$C_a = c\rho - L_f \rho_i \frac{\partial \theta_i}{\partial T} \quad \text{or} \quad C_a = c\rho + L_f \rho_w \frac{\partial \theta_w}{\partial T}. \quad (14)$$

This apparent heat capacity can replace the medium heat capacity term ( $c\rho$ ) in Eqs. (4) or (5) when the equations are intended to represent heat transport in soils that experience pore water phase change. Combining Eq. (14) with Eq. (11) and substituting  $\epsilon S_i$  for  $\theta_i$  yields the following apparent heat capacity term for freezing/thawing soils:

$$C_a = [(1-\epsilon)c_s \rho_s + \epsilon(1-S_w - S_i)c_a \rho_a + \epsilon S_w c_w \rho_w + \epsilon S_i c_i \rho_i] - \epsilon \rho_i L_f \frac{\partial S_i}{\partial T}. \quad (15)$$

Note that Eq. (15) will yield a higher heat capacity than Eq. (11) given that the derivative of the ice saturation with respect to temperature is negative in accordance with the soil freezing curve (Kurylyk and Watanabe, 2013).

### 3.7. Dimensionless numbers for subsurface heat transport

Conduction dominated systems can be found in regions of low groundwater velocity, such as in permafrost regions (Gold and Lachenbruch, 1973; Kane et al., 1991) or unfractured consolidated soil. Conversely, advective heat transport is often dominant in deep hydrothermal systems (Ingebritsen et al., 2006), in shallower saturated zones with high groundwater flow, and during episodic precipitation and snow melt events in the unsaturated zone (Taniguchi and Kayane, 1986; Tao and Gray, 1994; Zhao et al., 1997). Smith and Chapman (1983) demonstrated that the relative importance of the conductive or advective components of subsurface heat transfer is dependent on the water table relief, the hydraulic conductivity distribution and orientation, and the depth of flow. Due to spatial and temporal variations in temperature and water movement, the governing heat transport mode may also vary spatially and temporally (Koo and Kim, 2008).

In heat transport studies, the dimensionless Peclet number is the ratio of the advective heat flux (Eq. (2)) to the conductive heat flux (Eq. (1)):

$$P_e = \frac{q \rho_w c_w T}{\left( \lambda \frac{\partial T}{\partial x} \right)}. \quad (16)$$

Often, the temperature terms in Eq. (16) are canceled and the following form of the Peclet number is applied to determine which subsurface heat transport mode dominates (Domenico and Schwartz, 1990):

$$P_e = \frac{q \rho_w c_w L^*}{\lambda} \quad (17)$$

where  $L^*$  is a characteristic length (m). Understanding the appropriate selection of the Peclet number characteristic length is a recurring

problem in subsurface heat transport studies (van der Kamp and Bachu, 1989). The following Peclet number was proposed by Domenico and Palciauskas (1973) for basin scale transport where the velocity is unknown:

$$P_e^* = \frac{\rho_w^2 c_w k g B \Delta z}{2(\mu_w \lambda H)} \quad (18)$$

where  $B$  is the basin thickness (m),  $\mu_w$  is the dynamic viscosity of water (kg m<sup>-1</sup> s<sup>-1</sup>),  $k$  is the permeability of the soil matrix (m<sup>2</sup>),  $g$  is the acceleration of gravity (m s<sup>-2</sup>),  $\Delta z$  is the water table relief (m), and  $H$  is the horizontal basin dimension (m). Domenico and Palciauskas (1973) suggest that advection becomes significant when this version of the Peclet number is greater than 1. Other versions of the Peclet number for different hydrogeological scenarios were derived by van der Kamp and Bachu (1989) through dimensionless analysis.

The Stefan number is a dimensionless number that is often employed in cold regions subsurface heat transport studies. In the case of soil warming, the Stefan number ( $S_T$ ) is the ratio of the sensible heat required to warm a volume of homogeneous porous media from an initial temperature  $T_i$  (°C) to a final temperature  $T_f$  (°C) divided by the latent heat absorbed by the medium due to soil thawing. In hydrological nomenclature (i.e., volumetric saturations), the Stefan number is given as (Kurylyk et al., 2014b):

$$S_T = \frac{c\rho(T_f - T_i)}{L_f \rho_i \epsilon S_{ip}} \quad (19)$$

where  $S_{ip}$  refers to the ice saturation that undergoes phase change (i.e., thaws) over the interval of temperature change. At higher values of the Stefan number, sensible heat governs, and the thermal influence of phase change becomes less important.

In summary, groundwater flow and heat transport processes are interdependent and must be simulated in a coupled manner. Advection and conduction are the dominant modes of subsurface heat transport; however, the thermal effects of freezing and thawing can be significant in ephemerally freezing and thawing soils or in permafrost soils experiencing gradual thawing. Simulations can be greatly simplified if advective heat transport can be ignored, and the effect of ignoring advection can be analyzed in a preliminary fashion through the application of the Peclet number. Similarly, the governing equations for heat transport become simpler if the soil is not expected to experience freezing or thawing or if the moisture content is very low. The relative thermal effects of the latent heat of fusion can be investigated via the dimensionless Stefan number. At high Stefan numbers, simpler heat transport models that do not consider pore water phase change are appropriate. However, in the case of long term climate change, even high latitude soils that are perpetually frozen under the current climate (i.e.,  $S_{ip} = 0$  and  $S_T = \infty$  in Eq. (19)) may begin to thaw over time ( $S_{ip} > 0$ , and  $S_T$  is decreased). This thawing may drastically alter the hydraulic properties of the medium, activate groundwater flow, and consequently increase the Peclet number (Section 2). Thus the Peclet and Stefan numbers for characterizing heat transfer processes may both be strongly influenced by climate change in a particular subsurface environment.

Analytical solutions and numerical models can only provide answers to well-posed questions regarding the future thermal states of subsurface environments. Considerable care should be taken when selecting an appropriate governing equation for simulating the subsurface thermal response to decadal climate change. In general, model parsimony is preferred, especially for spatially extensive modeling, and a proper understanding of which heat transport processes may be ignored both for current and future climate conditions may greatly facilitate the modeling process.

#### 4. Analytical solutions to simplified heat transport equations

Many researchers have formulated analytical solutions to simplified heat transfer problems for domains only influenced by heat conduction and subject to different boundary conditions (e.g., Carslaw and Jaeger, 1959; Özi ik, 1980). Lunardini (1981, 1991) published multiple analytical solutions to simulate conductive heat transfer in cold regions with pore water phase change. Several analytical solutions that can be applied to predict the subsurface thermal response to climate change are discussed below.

##### 4.1. Analytical solutions to the conduction equation subject to surface temperature changes

Analytical solutions to the transient conduction equation have been proposed in the field of thermal geophysics for the inverse modeling of paleoclimates from borehole temperature–depth profiles (e.g., Mareschal and Beltrami, 1992; Beltrami et al., 1995; Bodri and Cermak, 2007; Lesperance et al., 2010). Other solutions have been developed for forward modeling the effects of future climate change on groundwater and soil temperature, assuming conduction is the only heat transport mechanism. For example, a solution to the transient conduction equation (Eq. (4)) with a future step change in surface temperature is provided by Williams and Smith (1989):

$$\text{Initial conditions : } T(z, t = 0) = T_0 + Gz \quad (20a)$$

$$\text{Boundary conditions : } T(z = 0, t) = T_0 + \Delta T \quad (20b)$$

$$\begin{aligned} \text{Analytical solution : } T(z = t) = T_0 + Gz \\ + \Delta T \left[ \operatorname{erf} \left( \frac{z}{\sqrt{4\alpha(t-\kappa)}} \right) - \operatorname{erf} \left( \frac{z}{\sqrt{4\alpha t}} \right) \right] \end{aligned} \quad (20c)$$

where  $T_0$  is the initial surface temperature ( $^{\circ}\text{C}$ ),  $\Delta T$  is the temporary step change in surface temperature ( $^{\circ}\text{C}$ ) that begins at  $t = 0$  and lasts until  $t = \kappa$  (s),  $G$  is the geothermal gradient ( $^{\circ}\text{C m}^{-1}$ ), and erf is the error function. The first erf term in Eq. (20c) is only included once  $t$  has exceeded  $\kappa$ . Superposition principles can be applied to modify Eq. (20c) to investigate the subsurface thermal influence of a series of previous or future shifts in the surface temperature boundary condition (Mareschal and Beltrami, 1992).

##### 4.2. Analytical solutions to the conduction–advection equation in a stable climate

Groundwater flow can also perturb temperature–depth profiles, as first described by Bullard (1939). Suzuki (1960) was the first to apply a solution to the transient conduction–advection equation (Eq. (5)) to examine how the upward or downward flow of water could significantly perturb subsurface temperature–depth profiles and how measured subsurface temperatures could be employed to infer groundwater flow rates. Stallman (1963) produced a more rigorous derivation of the transient conduction–advection equation and further discussed how analytical solutions to the equation could be used to infer groundwater velocity from temperature data. In a later classic publication, Stallman (1965) provided an exact solution to Eq. (5) subject to a harmonic boundary condition to account for seasonal or diurnal surface temperature variability. Velocity rates greater than  $2 \text{ cm d}^{-1}$  were detectable by analyzing observed groundwater temperature data with his analytical solution. Other researchers have developed variations of the solution provided by Stallman (1965) by considering different boundary conditions, steady state conditions (Bredenhoft and Papadopulos, 1965), and two-dimensional groundwater flow and/or heat transport (Domenico and

Palciauskas, 1973; Lu and Ge, 1996; Reiter, 2001). These solutions indicate that temperature–depth profiles are generally concave upward in areas of groundwater recharge and convex upward in areas of groundwater discharge as indicated in Fig. 4.

##### 4.3. Analytical solutions to the conduction–advection equation subject to long term surface temperature changes

Deviations from a linear temperature–depth profile can arise due to groundwater flow, thermal conductivity heterogeneities, or surface temperature variations due to climate or land cover change. Thus the causes of subsurface thermal anomalies can be difficult to distinguish (Kukkonen and Clauser, 1994; Kukkonen et al., 1994; Uchida et al., 2003; Ferguson and Woodbury, 2005; Ferguson et al., 2006). The combined subsurface thermal impacts of climate change and groundwater flow can be estimated using an analytical solution to the transient conduction–advection equation (Eq. (5)) subject to a temporally increasing surface temperature boundary condition. Taniguchi et al. (1999a) modified an analytical solution to the conduction–advection equation proposed by Carslaw and Jaeger (1959) and applied it to investigate the thermal evolution of subsurface environments with vertical groundwater movement and gradually increasing surface temperature:

$$\text{Initial conditions : } T(z, t = 0) = T_0 + Gz \quad (21a)$$

$$\text{Boundary conditions : } T(z = 0, t) = T_0 + \psi t \quad (21b)$$

Analytical solution

$$\begin{aligned} T(z = t) = T_0 + G(z - Ut) + \frac{1}{2U} (\psi + UG) \times \\ : \left[ (Ut - z) \times \operatorname{erfc} \left( \frac{z - Ut}{2\sqrt{\alpha t}} \right) + (Ut + z) \exp \left( \frac{Uz}{\alpha} \right) \operatorname{erfc} \left( \frac{z + Ut}{2\sqrt{\alpha t}} \right) \right] \end{aligned} \quad (21c)$$

where  $U$  is the thermal plume velocity due to pure advection ( $q_z c_w \rho_w / (c\rho)$ ,  $\text{m s}^{-1}$ ),  $G$  is the geothermal gradient ( $^{\circ}\text{C m}^{-1}$ ),  $T_0$  is the initial surface temperature ( $^{\circ}\text{C}$ ), erfc is the complementary error function, and  $\psi$  is the slope of the surficial temperature rise ( $^{\circ}\text{C s}^{-1}$ ). Taniguchi et al. (1999a) demonstrated how this analytical solution can be applied to determine groundwater fluxes from temperature profiles in regions of measured surface temperature rise. Similarly, if the groundwater flux and borehole temperatures are known, the solution can be inverted to reproduce surface temperature history if it is assumed to follow a linear pattern.

This solution has been applied in several studies in Japan to investigate the relationships between groundwater flow, surface temperature changes, and subsurface temperature–depth profiles (Miyakoshi et al., 2003; Taniguchi et al., 2003; Uchida and Hayashi, 2005). Recently, Gunawardhana and Kazama (2011) applied Eq. (21c) to predict the effects of future climate change on subsurface temperature in the Sendai Plain, Japan using 18 climate scenarios for the period 2060–2099. Their results indicated a rise (1.2–3.3  $^{\circ}\text{C}$ ) in aquifer temperature at a depth of 8 m. Fig. 5 shows the simulated temperature–depth profiles for a hypothetical warming scenario generated with the solution by Taniguchi et al. (1999a).

Kumar et al. (2012) modified the solution by Taniguchi et al. (1999a) by incorporating a mixed Robin type boundary condition that enables the user to specify air temperature rather than ground surface temperature for the upper boundary condition, as it is typically easier to obtain air temperature data than surface temperature data. Kurylyk and MacQuarrie (2014) derived an analytical solution to the conduction–advection solution that is more flexible than Eqs. (21a), (21b), and (21c) because exponential terms are included in both initial and boundary conditions. These exponential terms allow the user to match present-day non-linear temperature depth profiles (initial conditions)

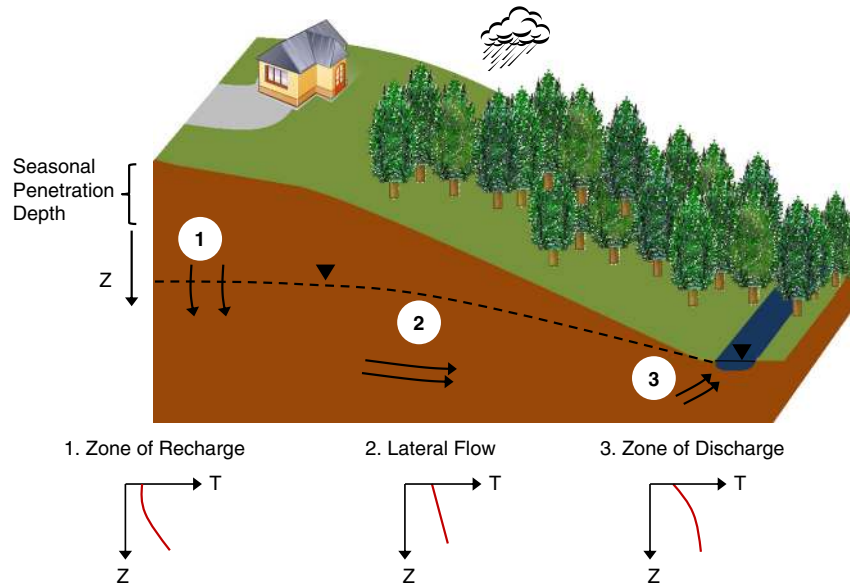


**Fig. 4.** Temperature depth profiles in a stable climate as a function of the groundwater flow direction. Below the seasonal penetration depth, temperature–depth profiles are concave upward in recharge areas (vertical downward flow), linear in lateral flow regions (assuming no horizontal temperature gradient), and convex upward in discharge areas (vertical upward flow) (from Kurylyk and MacQuarrie, 2014). Figure reproduced with permission.

and non-linear climate model projections (boundary condition). Thus, this solution can be directly applied to forward model the evolution of present-day temperature profiles exhibiting curvature (e.g., due to vertical groundwater flow or past climate change), whereas Eq. (21c) requires intermediate steps due to the assumed linear initial

conditions. Kurylyk and MacQuarrie (2014) employed this solution to demonstrate that zones of groundwater recharge will experience accelerated groundwater temperature warming due to climate change because of the parallel heat conduction and advection from the ground surface.

Finally, Taniguchi et al. (1999b) employed a slightly modified version of Eq. (21c) that considers a sudden and permanent increase in the surface temperature rather than a gradual increase. Menberg et al. (2014) demonstrated that the solution form could be superimposed to simulate subsurface thermal evolution due to a series of  $n$  climate regime shifts at the ground surface:

— Time = 0 yr      — Time = 20 yr  
 — Time = 40 yr      — Time = 60 yr  
 — Time = 80 yr      — Time = 100 yr

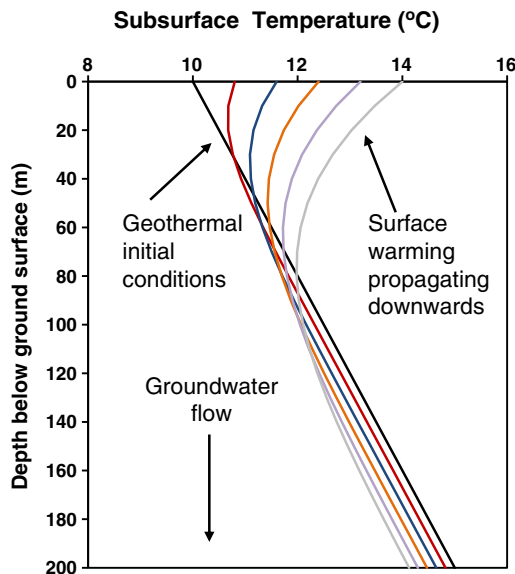


**Fig. 5.** Climate change-induced evolution of temperature–depth profiles in hydrogeologically active subsurface environments generated from the solution by Taniguchi et al. (1999a). The initial surface temperature was assumed to be 10 °C, the geothermal gradient was a typical 0.025 °C m<sup>-1</sup>, and the warming scenario was 0.04 °C yr<sup>-1</sup> ( $\psi$ , Eq. (21b)). The thermal properties were taken from Table 2 (saturated sand). A vertical Darcy recharge flux of 0.25 m yr<sup>-1</sup> was assumed; thus, this figure represents Zone 1 of Fig. 4.

$$\text{Initial conditions : } T(z, t = 0) = T_0 \quad (22a)$$

$$\text{Boundary conditions : } T(z = 0, t) = T_0 + \sum_{i=1}^n \Delta T_i \cdot H(t - t_i) \quad (22b)$$

$$\text{Solution : } T(z = t) = T_0 + \sum_{i=1}^n \frac{\Delta T_i}{2} \cdot \left\{ \operatorname{erfc} \left( \frac{z - U(t - t_i)}{2\sqrt{\alpha(t - t_i)}} \right) + \exp \left( \frac{Uz}{\alpha} \right) \cdot \operatorname{erfc} \left( \frac{z + U(t - t_i)}{2\sqrt{\alpha(t - t_i)}} \right) \right\} \cdot H(t - t_i) \quad (22c)$$

where  $\Delta T_i$  (°C) is a shift in the surface boundary condition occurring at time  $t_i$  (s) in comparison to the surface temperature immediately preceding  $t_i$  and  $H$  is the Heaviside step function. The Heaviside terms in Eqs. (22b), and (22c) indicate that there is no surface or subsurface thermal influence of a particular surface temperature shift  $\Delta T_i$  until the time  $t$  exceeds the timing of that particular shift  $t_i$ . The exact solution form given in Eq. (22c) is not well suited for studying deeper subsurface temperature evolution as no geothermal gradient is included in the initial conditions. Menberg et al. (2014) applied this solution to forward model the influence of post 1970 climate regime shifts on groundwater temperature in shallow wells in Germany. Observed increases in groundwater temperature from 1970 to 2000 generally matched the groundwater temperature increases predicted with Eq. (22c).

4.4. Analytical solutions for subsurface heat transport with freezing and thawing

The first mathematical treatises on heat transport with freezing and thawing were conducted in the late 1800's by Stefan and Neumann, who studied the freezing and thawing of bulk ice (Lunardini, 1981). Their solutions have since been adapted by geotechnical engineers and permafrost hydrologists to predict the seasonal depth of thawing (active layer in permafrost soils) or freezing (frost depth in ephemerally freezing soils) (e.g., Jumikis, 1966). Where applicable, these solutions have herein been presented in a modified form to be consistent with the nomenclature (e.g., water saturations and mass-based latent heat) previously presented. The Neumann and Stefan equations are presented for the case of thawing, rather than freezing, as this will be the dominant effect produced by climate change.

A modified form of the classical analytical Neumann solution has been employed by numerous researchers simulating heat transport in cryogenic soils (Lunardini, 1981). This solution ignores advective heat transport but accounts for conduction and latent heat released or absorbed during freezing or thawing. The soil medium is treated as a semi-infinite domain initially at some uniform temperature  $T_i$  (°C) below the freezing temperature  $T_f$  (°C). The surface temperature  $T_s$  (°C) is then instantaneously raised to some temperature above the freezing temperature. The medium is discretized into thawed and frozen layers which are separated at a thawing interface and are characterized by different thermal properties. The depth to this thawing interface  $X$  (m) will increase with time (Fig. 6). The following form of the Neumann solution was modified from Jumikis (1966) and Harlan and Nixon (1978) assuming that  $T_f = 0$  °C:

$$X(t) = m\sqrt{t} \tag{23}$$

where  $X$  is the depth to the thawing front (m) (Fig. 6),  $m$  is the coefficient of proportionality ( $m\text{ s}^{-0.5}$ ), and  $t$  is the time (s). The  $m$  parameter can be determined by equating  $Y_1$  and  $Y_2$ :

$$Y_1 = f(m) = 0.5L_f\rho_iS_{ip}\varepsilon\sqrt{\pi}m \tag{24}$$

$$Y_2 = \frac{\lambda_u}{\sqrt{\alpha_u}}(T_s) \left[ \exp\left(\frac{-m^2}{4\alpha_u}\right) / \text{erf}\left(\frac{m}{2\sqrt{\alpha_u}}\right) \right] - \frac{\lambda_f}{\sqrt{\alpha_f}}(T_i) \times \left[ \exp\left(\frac{-m^2}{4\alpha_f}\right) / \text{erfc}\left(\frac{m}{2\sqrt{\alpha_f}}\right) \right] \tag{25}$$

where  $\alpha_f$  and  $\alpha_u$  are the bulk thermal diffusivities of the frozen and unfrozen soil respectively ( $\text{m}^2\text{ s}^{-1}$ ),  $\lambda_f$  and  $\lambda_u$  are the bulk thermal conductivities of the frozen and unfrozen soil respectively ( $\text{W m}^{-1}\text{ °C}^{-1}$ ), and other terms have been previously defined. The temperature distributions in the thawed and frozen zones can also be obtained from the Neumann solution (Jumikis, 1966; Lunardini, 1981). The Neumann solution can theoretically be applied to simulate permafrost degradation due to rising surface temperature. However, the step change in surface temperature is not very representative of climate change-induced surface temperature trends and could be better applied in the case of land cover change in permafrost landscapes.

Stefan's formula is an even simpler approach to the problem of soil thawing (Jumikis, 1966; Harlan and Nixon, 1978). The  $m$  term (Eq. (23)) can be easily obtained if it is assumed that the temperature-

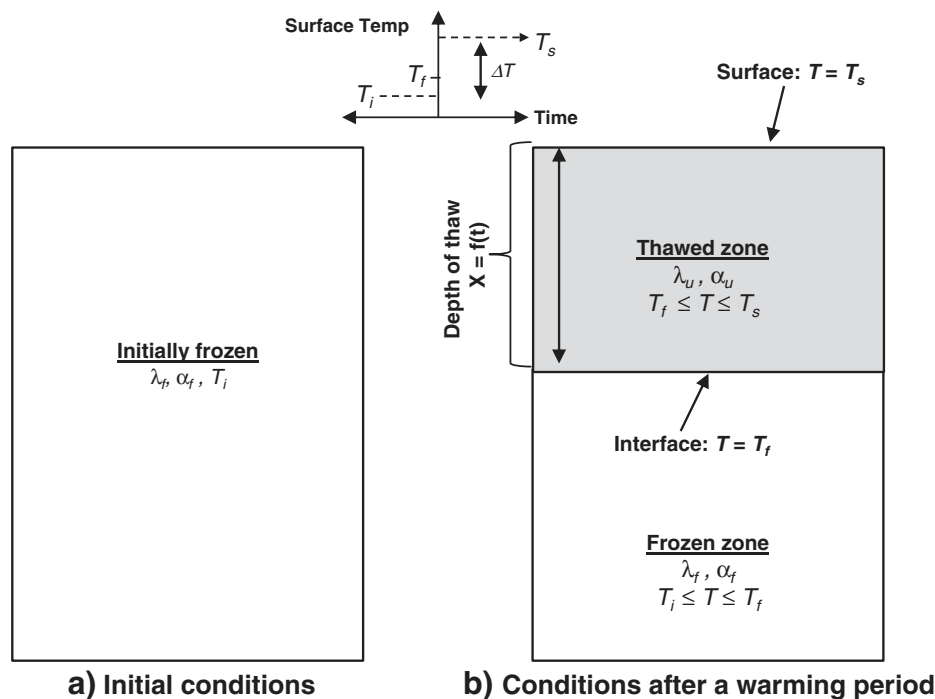


Fig. 6. The theoretical conditions for the Neumann solution at (a) time = 0, and (b) after a period of thawing. The depth to the frozen/unfrozen interface  $X$  increases with time. The temperature at the freeze–thaw interface is  $T_f$  (after Nixon and McRoberts, 1973; Kurylyk et al., 2014b). The frozen and unfrozen zones are characterized by different thermal properties. This figure also represents the conditions for the Stefan solution when  $T_i = T_f$ .

depth profile in the thawed zone is linear (i.e., at steady-state), and the initial temperature is  $0\text{ }^{\circ}\text{C}$ :

$$X(t) = m\sqrt{t} = \sqrt{2S_T\alpha t} = \sqrt{\frac{2\lambda_u T_s t}{L_f \rho_i \varepsilon S_{ip}}} \quad (26)$$

The Stefan solution is an approximate mathematical solution due to the assumed steady-state thermal conditions in the continuously expanding thawed zone. The solution accuracy can be shown to be inversely related to the Stefan number via a comparison to the exact Neumann solution (Kurylyk et al., 2014b), and the solution errors are often reasonably small at typical Stefan numbers for thawing soils. Smaller Stefan numbers imply that latent heat is governing and that the thawing front propagation will be slow, thus allowing the thawed zone temperature distribution to approach steady-state.

The errors noted by Kurylyk et al. (2014b) are errors associated with the mathematical solution development (i.e., due to the contradictory steady-state assumption) and thus do not address how well the solution represents soil freezing physics at a particular site. There are other conditions of the Stefan solution that may not adhere to physical processes, including the step function soil freezing curve (i.e., freezing occurs completely at  $T_f$  rather than over a finite temperature range), homogeneous soil thermal properties, and initial temperatures close to  $0\text{ }^{\circ}\text{C}$ . Like the Neumann solution, another limitation of the application of the Stefan solution for climate change sensitivity studies is that a step change is not a realistic representation of climate model-projected increases in surface temperature.

Adaptations of the Stefan solution have been proposed for simulating soil thawing accounting for different boundary conditions and thermal property heterogeneities (e.g., Aldrich and Paynter, 1953; Lock et al., 1969; Nixon and McRoberts, 1973; Cho and Sunderland, 1974; Lunardini, 1981; Hayashi et al., 2007; Changwei and Gough, 2013). For example, as Harlan and Nixon (1978) note, the product of  $T_s$  and  $t$  in Eq. (26) is essentially the integral of the surface temperature–time function. This fact can be used to obtain a more general approximate Stefan equation that can accommodate a variety of surface temperature functions:

$$X(t) = \sqrt{\frac{2\lambda_u I_{th}}{L_f \rho_i \varepsilon S_{ip}}} \quad (27)$$

where the surface thawing index  $I_{th}$  ( $^{\circ}\text{C s}$ ) is essentially the temporal integral of the surface temperature function (from time = 0 to  $t$ ), provided that the function is continuously above the freezing temperature (Harlan and Nixon, 1978). If the thawing index was computed using air temperature rather than surface temperature, an additional  $n$  factor equal to the ratio between ground surface temperature and air temperature is placed in the numerator under the radicand in Eq. (27) (Harlan and Nixon, 1978; Klene et al., 2001). Often this equation is further simplified using empirical coefficients that can be calibrated to site conditions (Hinkel and Nicholas, 1995; Nelson et al., 1997; Anisimov et al., 2002). Other slightly more complex analytical or semi-analytical equations (Freitag and McFadden, 1997; Riseborough et al., 2008; Zhang et al., 2008a) have been developed for simulating the depth of thaw, but the most common analytical equation that has been used in permafrost models is the Stefan equation (Riseborough et al., 2008).

The latent heat associated with pore water phase change increases the effective heat capacity of frozen soil and makes it less responsive to surficial climate change. Thus, permafrost soils are characterized by warming retardation compared to temperate soils experiencing the same surficial warming rate. We propose a thaw retardation factor  $R_{th}$  that is equal to the total energy (sensible heat plus latent heat) required to warm a unit volume of frozen soil from an initial uniform temperature  $T_i$  to a uniform temperature above freezing  $T_j$ , divided by the sensible heat

required to warm the same volume of unfrozen soil by a change in temperature equal in magnitude to  $T_j - T_i$ :

$$R_{th} = \frac{L_f \rho_i \varepsilon S_{ip} + c\rho(T_j - T_i)}{c\rho(T_j - T_i)} \quad (28)$$

Note that this is not simply the inverse of the Stefan number (Eq. (19)) as the sensible heat component is included in both numerator and denominator of Eq. (28). Soils with lower porosities and/or initial ice saturations will respond more rapidly to surficial thermal perturbations than high porosity, ice-saturated soils, as considerable energy can be consumed during phase change.

The addition of the phase change term in the governing heat transport equation adds mathematical complexity due to the inclusion of a moving boundary (freeze–thaw interface). To our knowledge, only two attempts have been made to derive exact analytical solutions that include conduction, advection, and phase change. Nixon (1975) and Lunardini (1998) provided exact solutions to a transient conduction–advection equation subject to phase change, but both solutions are only valid if the groundwater velocity is proportional to the rate of the thawing front penetration. Kurylyk et al. (2014b) detailed a complete derivation of an approximate solution listed by Lunardini (1998) that considers conduction, advection, and phase change. Like the Stefan solution, this solution is accurate at lower Stefan numbers when the temperature distribution in the thawed zone can be assumed to be close to steady-state. It should also be noted that analytical solutions that ignore phase change and advection may still be applicable for simulating the thermal response of permafrost to climate change provided that the soil moisture content is very low (Harlan and Nixon, 1978), or that the degree of warming is insufficient to produce soil thawing (Gold and Lachenbruch, 1973).

There are many limitations associated with the analytical solutions presented above. For example, analytical solutions typically assume one dimensional flow and heat transport, spatiotemporally invariant groundwater flow, homogeneous and isotropic thermal properties, constant pore water phase (except for the few examples noted above), and simplified boundary conditions (e.g., linear rise or step increase in surface temperature). Although, analytical solutions are limited in their ability to simulate subsurface heat transport processes in complex hydrogeological environments, the recent resurgence of papers employing analytical solutions to study groundwater temperature evolution due to climate change (e.g., Gunawardhana and Kazama, 2011; Gunawardhana et al., 2011; Kurylyk and MacQuarrie, 2014; Menberg et al., 2014) suggests that analytical solutions have not been completely abandoned in favor of numerical models. Analytical solutions are still useful for benchmarking numerical models (Kurylyk et al., 2014b), performing quick analyses of idealized systems (Kurylyk and MacQuarrie, 2014), and obtaining first order approximations of future groundwater temperature evolution in natural environments (Gunawardhana and Kazama, 2011; Menberg et al., 2014). The continued use of analytical solutions for simulating subsurface heat transport phenomena is due, in part, to the fact that natural variations in the thermal conductivity of geological media are orders of magnitude smaller than natural variations in hydraulic conductivity (e.g., Domenico and Schwartz, 1990), and thus homogeneous assumptions are better justified than in the case of analytical solutions of groundwater flow.

## 5. Numerical models of groundwater flow and heat transport

As a result of the limitations associated with analytical solutions, many groundwater flow and heat transport studies have employed numerical solution methods. These methods are flexible and can accommodate soil heterogeneities, varying boundary conditions, pore water phase change, and multi-dimensional groundwater flow and energy transport.

### 5.1. Early numerical modeling of groundwater flow and heat transport

Studies of the effects of groundwater flow on subsurface thermal regimes in complex hydrogeological environments first emerged in the 1970s and 1980s with the development of finite difference and finite element numerical models (Parsons, 1970; Sauty et al., 1982; Smith and Chapman, 1983; Woodbury and Smith, 1985; Forster and Smith, 1989). Many of these early studies provided a better understanding of the relationship between complex groundwater flow patterns and subsurface thermal conditions. For example, Smith and Chapman (1983) created a two-dimensional Galerkin finite element model of groundwater flow and heat transport processes in a regional flow system. They found that the transition from conduction to advection-dominated regimes was sharp and that advection was significant in highly permeable regions with high topographic relief. Woodbury and Smith (1985) developed a three-dimensional advection/conduction model and evaluated the impacts of multiple hydrogeological scenarios on subsurface thermal regimes. Forster and Smith (1989) highlighted the limitations of previous one-dimensional analyses and discussed the influences of topography, permeability, recharge, free convection, and fracture zones on subsurface thermal environments.

### 5.2. Contemporary groundwater flow and heat transport models

Over the past two decades, a few numerical models of groundwater flow and heat transport with user-friendly graphical user interfaces (GUIs) have become publicly available and widely utilized. For example, VS2DH (Healy and Ronan, 1996; Hsieh et al., 2000) is a multi-dimensional finite difference model developed by the U.S. Geological Survey, which has been frequently employed to simulate energy and water exchanges between aquifers and surface water bodies (e.g., Barlow and Coupe, 2012; Voytek et al., 2014). SUTRA is a three-dimensional, density-dependent, finite element model developed by the U.S. Geological Survey (Voss, 1984; Voss and Provost, 2010) that has been widely applied in groundwater flow and heat or solute transport studies (e.g., Bundschuh, 1993; Burow et al., 2005; McKenzie et al., 2006, 2007; Ge et al., 2011). FEFLOW is another three dimensional, density-dependent, finite element groundwater flow and heat transport model (Diersch, 2014) that is well-documented and has been frequently utilized to study subsurface thermal processes (e.g., Trefry and Muffels, 2007; Bridger and Allen, 2010; Diersch et al., 2011). A powerful model that has recently emerged is HydroGeoSphere (Goderniaux et al., 2009; Brunner and Simmons, 2012; Therrien et al., 2012), which is a fully-integrated control-volume finite element model that simulates two-dimensional overland flow and three-dimensional subsurface flow and energy transport. Surface processes (e.g., evaporation and transpiration) are also accommodated in HydroGeoSphere, which removes the need to drive subsurface models with surface model output.

### 5.3. Groundwater flow and heat transport models that include freeze–thaw

The publicly available versions of most existing groundwater flow and heat transport models that include a GUI are not capable of simulating the effects of cryogenic processes on groundwater flow and energy transport. However, modeling pore water freeze–thaw has been shown to improve comparisons between simulated thermal results and field data for permafrost regions or ephemerally freezing soil (Luo et al., 2003).

Numerical groundwater flow and energy transport models that accommodate cryogenic processes typically simulate the interactions between temperature, pressure, and ice or water saturations on the basis of thermodynamics using a form of the Clapeyron equation (Hansson et al., 2004; Zhang et al., 2007; Dall'Amico et al., 2011; Liu and Yu, 2011; Tan et al., 2011; Gouttevin et al., 2012). Often, the 'freezing = drying' assumption is employed for saturated conditions, in which the soil water freezing curve (SFC, unfrozen water content versus temperature) is related to a soil water characteristic curve

(SWCC) through capillary theory coupled to the Clapeyron equation (Koopmans and Miller, 1966; Spaans and Baker, 1996; Kurylyk and Watanabe, 2013).

The relationship between permeability and ice content is often determined empirically from laboratory measurements or theoretically derived from classical unsaturated relative permeability functions. Usually it is first assumed that ice has a similar effect as pore air in lowering permeability (e.g., McKenzie et al., 2007; Bense et al., 2009; Tan et al., 2011; Gouttevin et al., 2012). Then, an empirical impedance term (e.g., Jame and Norum, 1980) is often included to account for the apparent reduction in hydraulic conductivity caused by pore ice formation in comparison to pore air entry, but the utility of this impedance function has been questioned (Newman and Wilson, 1997). Further discussion on the mathematical representation of freeze–thaw processes in unsaturated porous media, particularly with respect to the development of the soil freezing curve and permeability function, can be found in Kurylyk and Watanabe (2013).

Harlan (1973) is credited for developing the first coupled groundwater flow and heat transport model that incorporated the effects of freezing and thawing. In this one-dimensional, finite-difference model, the migration of soil moisture was simulated with a Darcian hydraulic approach, which contrasted strongly with the capillary models employed by those studying frost heave phenomena (e.g., Miller, 1972; 1980). Harlan's (1973) contribution was followed by several other one-dimensional models of water flow and heat transport in freezing soils. These models made improvements in relating the SWC to the SFC and in attempting to establish a physically-based relationship between ice content and hydraulic conductivity (Guymon and Luthin, 1974; Taylor and Luthin, 1978; Flerchinger and Saxton, 1989; Newman and Wilson, 1997; Shoop and Bigl, 1997; Zhao et al., 1997; Hansson et al., 2004; Zhang et al., 2007; Kahimba et al., 2009). Numerous other examples of models that account for the effects of freezing and thawing are given by Li et al. (2010); however, these models are typically one-dimensional, and the source codes are often not publicly available.

Recently, multi-dimensional water flow and energy transport models have emerged that are capable of accommodating freeze–thaw processes. Ippisch (2001) developed a rigorous three-dimensional groundwater flow and energy transport model to simulate coupled water, heat, gas, and solute transport in permafrost soils. McKenzie et al. (2007) presented modifications to the SUTRA code to include the effects of freezing and thawing on water and energy transport within the saturated zone. Their contribution was the first to document freeze–thaw modifications to a widely adopted variable-density, multi-dimensional groundwater flow and energy transport model. Dall'Amico et al. (2011) presented a robust model that accommodates variably-saturated freeze–thaw processes using a form of Richards' equation. The model was successfully tested against the Neumann solution and experimental data. Painter (2011) developed the three phase numerical model MarsFlo to simulate heat and moisture migration in variably saturated, partially frozen media. MarsFlo simulations compared favorably with results from the Neumann solution and experimental data (unfrozen water content) collected by Jame and Norum (1980) and Mizoguchi (1990). MarsFlo was originally developed for simulating Martian hydrology (Grimm and Painter, 2009; Painter, 2011), but Frampton et al. (2011, 2013) have recently applied it to study terrestrial permafrost processes.

Another recently-developed cryohydrogeological model was applied to assess potential designs of the Galongla tunnel in Tibet (Tan et al., 2011). The governing groundwater flow equation in this unnamed model was altered to accommodate the Soret effect (moisture redistribution during freezing). Model simulations concurred with the laboratory experiments of Mizoguchi (1990). Liu and Yu (2011) coupled a modified version of Fourier's law that included convection and a source term for freezing and thawing with Richard's equation and the mechanical constitutive relationship to simulate the flow of energy, water, and stress in freezing soils. Results from the model simulations compared

favorably to measured moisture and temperature distributions under pavement.

ARCHY is an emerging cryohydrogeological model developed at Los Alamos National Laboratory (LANL) for simulating variably-saturated water, energy and solute transport in permafrost environments (Rowland et al., 2011). ARCHY was developed by integrating two previous models: MAGNUM (Barnhart et al., 2010) and TRAMP (Travis and Rosenberg, 1997). Rowland et al. (2011) performed simulations with ARCHY to demonstrate the importance of advective heat transport in the formation of taliks below lakes. Two other ongoing projects at LANL are the development of the Arctic Terrestrial Simulator (ATS, Coon et al., 2012) and PFLOTRAN (Karra et al., 2014), which perform simulations in parallel computational environments and will facilitate the investigation of cold regions subsurface hydrological processes at greater spatiotemporal resolution.

Recently, Endrizzi et al. (2013) have produced the open source software package GEOTop 2.0, which is a powerful simulator of energy and moisture fluxes across the surface and within the subsurface and accounts for the dynamic freeze–thaw process in soils. Considered surface processes include snowpack accumulation and melt and turbulent and radiative energy fluxes. GEOTop 2.0 allows for three dimensional heat and water transport within the subsurface in accordance with Richards equation, and the subsurface freezing and thawing routines are based on the work by Dall'Amico et al. (2011). Notably, GEOTop 2.0 removes the need for cold regions groundwater flow and energy transport models to be driven at the boundary with surface model output (e.g., infiltration and ground surface temperature).

Despite the recent advances in cryohydrogeological numerical codes, most of these powerful simulators have not yet been incorporated into publicly available products with a user-friendly GUI. These models are often very distinct from one another both in terms of their underlying theory and the nomenclature employed (Kurylyk and Watanabe, 2013), thus a remaining challenge is the development of appropriate benchmarks to form inter-code comparisons (Kurylyk et al., 2014b).

## 6. Simulated climate change impacts on groundwater flow and heat transport in cold and temperate regions

The emergence of the groundwater flow and heat transport models discussed above has enabled researchers to investigate the subsurface thermal response to climate change in hydrogeologically complex environments. Three of the studies that have employed numerical models to investigate the interrelationships between groundwater flow, climate change, and subsurface thermal regimes were conducted for relatively warm regions. Uchida et al. (2003) used a three-dimensional groundwater flow and heat transport model (MODFLOW coupled to MT3D) to compare the relative subsurface thermal effects (e.g., deviation from a linear temperature–depth profile) of groundwater flow and a linear surface temperature increase of  $0.02\text{ °C yr}^{-1}$ . They found that in discharge regions, the thermal effects due to groundwater flow can dominate the thermal perturbations due to increased surface temperatures. Bense and Kooi (2004) found that groundwater flow and heat transport simulations of the Peel Boundary Fault in the Netherlands were improved if recent measured climate change was incorporated into the boundary conditions. Gunawardhana and Kazama (2012) used climate projections for the Sendai Plain, Japan, derived from five GCMs and three emission scenarios to drive one-dimensional VS2DH groundwater flow and heat transport simulations with a very coarse temporal resolution (1 year). They found a range (1.0–4.28 °C) of simulated increases in groundwater temperature at a depth of 8 m.

Because of the potential hydrological and ecological ramifications of permafrost degradation and the accelerated observed warming at high latitudes (Section 2), the majority of the recent studies investigating climate change-induced subsurface warming have been conducted for cold regions. Bense et al. (2009) used a finite element solution (FlexPDE

software) to a two-dimensional form of the transient conduction–advection equation with freeze–thaw to examine the potential impact of a  $0.03\text{ °C yr}^{-1}$  warming trend in permafrost regions. Their simulations demonstrated that permafrost degradation due to surface warming will likely establish groundwater flow paths and activate dormant groundwater flow systems (e.g., Fig. 2). Frampton et al. (2011) applied a linearly increasing upper thermal boundary ( $0.01\text{ °C yr}^{-1}$ ) to drive subsurface energy transport simulations with MarsFlo and demonstrated that climate change may decrease the seasonal variability of groundwater discharge in permafrost regions. Ge et al. (2011) utilized SUTRA to simulate groundwater and surface water exchange due to seasonal and decadal ( $0.03\text{ °C yr}^{-1}$ ) air temperature variations in the Tibet Plateau, China. The results showed that the active layer could increase in thickness by a factor of three within 40 years and that the resultant increase in permeability and aquifer thickness could similarly increase groundwater discharge by a factor of three. Jiang et al. (2012b) used the modified version of Hydrus (Hansson et al., 2004) to investigate the impact of 21st century climate change on active layer thickness. They simulated a future active layer thickness of 3 m in a boreal site and 1 m in a tundra site, which were significantly greater than predictions from previous studies that had assumed conduction was the only important heat transport mechanism.

Bense et al. (2012) simulated the hydrogeological response of permafrost to a warming climate in an idealized sedimentary basin with the undulating hill slope described by Tóth (1963). They suggested that the subsurface hydraulic response to climate change could be characterized by increased aquifer permeability due to permafrost degradation and uptake of water from increased heads in sub-permafrost aquifers. For the hydrogeological environment they considered, advective heat transport did not accelerate permafrost thaw under typical recharge rates. However, they suggested that advective transport could still impact permafrost degradation rates if recharge rates were not limited by precipitation (e.g., sourced by a draining surface water body), the groundwater flow was focused, or geothermal heat flow anomalies occurred. Grenier et al. (2013) applied a coupled heat and water transport model with phase change to investigate the effect of glaciation cycles on groundwater flow patterns in an idealized river–plain system with sub-river taliks. They demonstrated that the size of the river was the major control of talik evolution but that groundwater flow could also affect these processes.

Sjöberg et al. (2013) applied three warming scenarios ( $0.5\text{ °C yr}^{-1}$ ,  $0.1\text{ °C yr}^{-1}$ ,  $0.05\text{ °C yr}^{-1}$ ) to simulate a two-dimensional cryohydrogeological system in MarsFlo and showed that permafrost degradation occurred along the upper (i.e., ground surface) and seepage face boundaries of their modeling domain. They also noted that although the subsurface temperatures responded quickly to the surficial thermal perturbations, there was a lag in the melting of subsurface ice. The  $0.5\text{ °C yr}^{-1}$  warming scenario employed by Sjöberg et al. (2013) certainly exceeds the most extreme warming projections produced by any climate model. Frampton et al. (2013) applied MarsFlo to investigate the subsurface thermal and hydraulic response to the same three warming trends as Sjöberg et al. (2013). The model results indicated that intra-annual river flow variability would decrease under warming scenarios and that this phenomenon may be an indicator of permafrost degradation. They also found that groundwater discharge and river flow may decrease following the complete degradation of permafrost.

McKenzie and Voss (2013) employed SUTRA to demonstrate the effects of permafrost degradation in a Tóthian groundwater flow regime. They found that the significance of advective heat transport is dependent on the surficial topography, hydrogeologic heterogeneity and anisotropy, and the permeability of the groundwater flow system. Their simulations suggested that advective heat transport could reduce the time to complete permafrost degradation by one-third compared to the timing for permafrost degradation in the absence of advection (i.e., conduction-only). The influence of advective heat transport on

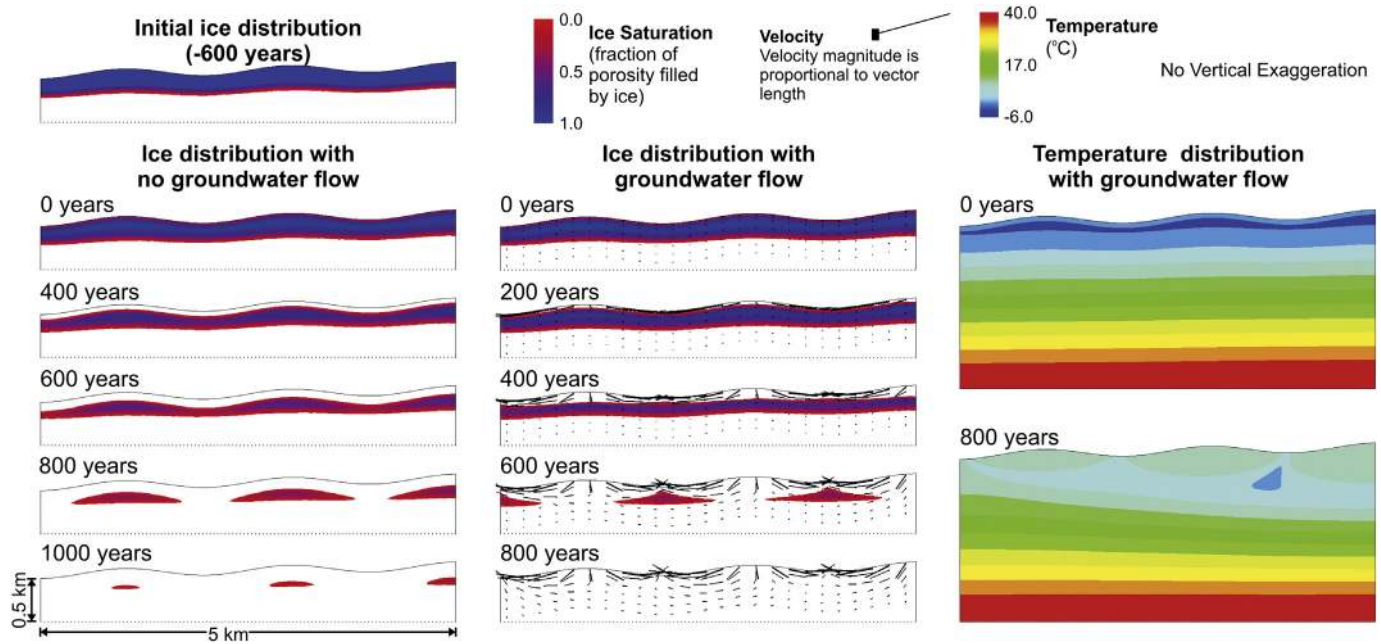


Fig. 7. Comparison of the timing and pattern of conduction-dominated and advection-influenced permafrost thaw (from McKenzie and Voss, 2013). The simulated evolution of ice distribution is shown without (left pane) and with (center pane) the effects of advective heat transport. The warming rate was  $0.01\text{ }^{\circ}\text{C}\cdot\text{yr}^{-1}$ . Permafrost degradation occurs first in the valleys for conduction-dominated thaw, but under the hills for advective-influenced thaw. The simulated thermal evolution when the effects of advective heat transport were considered is shown on the right pane. More details concerning the modeling can be found in McKenzie and Voss (2013). Figure reproduced with permission.

the pattern of permafrost thaw was also investigated (Fig. 7). They further demonstrated that intra-permafrost groundwater flow can accelerate permafrost thaw.

Kurylyk et al. (2014a) applied a modified version of SUTRA that allows for freezing in variably saturated soils to investigate the influence of climate change on the timing, magnitude, and temperature of groundwater discharge from shallow aquifers experiencing seasonal freeze–thaw. Seven downscaled climate scenarios for eastern Canada were employed to drive surface models to produce future groundwater recharge and ground surface temperature trends, and the results from the surface models were utilized to form the surface boundary conditions in SUTRA. The simulations indicated that the thermal regimes of shallow aquifers are not as resilient to climate change as previous thought, and that their thermal sensitivity may depend on the aquifer configuration.

Briggs et al. (2014) utilized the same modified version of SUTRA to simulate mechanisms for observed permafrost aggradation in the periphery of a receding lake in a discontinuous permafrost region in Alaska, USA. Their simulations demonstrate that the permafrost formation was likely due primarily to the shading caused by emerging shrubs and to a lesser degree by reduced groundwater recharge (heat advection) during the summer months due to increased transpiration. They further demonstrated that the new permafrost will eventually thaw (likely within seven decades) based on the climate projections for that location.

In summary, recent advances in numerical models have enabled researchers to simulate complex thermal hydrogeological processes for a variety of climate change scenarios. In general, researchers have demonstrated that subsurface thermal and hydrologic regimes will respond to climate-induced surficial perturbations in temperature. The majority of these studies have been conducted for permafrost regions, and they have suggested that advective heat transport has the potential to significantly increase the rate of permafrost thaw, which will lead to activated aquifers and changing surface and subsurface hydrological conditions.

## 7. Discussion and conclusions

The body of knowledge on the subsurface thermal impacts of climate change is expanding. However, there are still many gaps in existing research. The following section discusses these gaps and the opportunities for improvements and expansion in future studies.

### 7.1. The role of advective heat transport in accelerating permafrost thaw

The majority of studies that have simulated future permafrost degradation and/or variations in active layer thickness invoked the assumption that conduction is the only significant mode of heat transport in cold regions. Broad, unsubstantiated statements regarding the insignificance of advective heat transport in cryogenic soils can still be found in current literature. Admittedly, this simplification is often likely required to reduce simulation time due to the large-scale nature of many of these studies. However, several field and modeling studies (Kane et al., 2001; Frampton et al., 2011; Ge et al., 2011; Hasler et al., 2011; Rowland et al., 2011; Westermann et al., 2011; de Grandpre et al., 2012; Jiang et al., 2012b; McKenzie and Voss, 2013; Wellman et al., 2013) have demonstrated that advective heat transport can still be significant in certain permafrost environments. The degree to which advective heat transport plays a role in permafrost degradation may depend on many factors such as the proximity to surface water bodies, the timing and magnitude of precipitation, local and regional topography, and the existence and distribution of taliks. Further study is needed to attempt to quantify the impact of advective heat transport for a range of climatic, hydrogeological, and surficial conditions. As previously detailed, increasingly sophisticated models that can accommodate groundwater flow and heat transport with freezing and thawing are now becoming available. These models can be utilized to develop a more comprehensive framework for identifying scenarios when advective transport will impact permafrost dynamics and investigating the associated implications for the timing of large-scale



permafrost thaw and carbon release (e.g., Kane et al., 1991; Zhang et al., 2003; Noetzli et al., 2007; Zhang et al., 2008b; Etzelmüller et al., 2011; Wisser et al., 2011; Guo et al., 2012; Hipp et al., 2012; Jafarov et al., 2012; Lawrence et al., 2012; Streletskiy et al., 2012).

### 7.2. Emerging datasets for model assessment

Most studies investigating the cryohydrogeological implications of climate change have assumed idealized aquifers, but very few field-based studies exist to corroborate the general predictions obtained from idealized settings. Ireson et al. (2013) stated: 'modeling of field-scale behavior represents a major challenge, even while physically-based models continue to improve. It is suggested that progress can be made by combining well-designed field experiments with modeling studies.' Traditionally, there has been a lack of field data available to accomplish this purpose. However, Minsley et al. (2012) have recently produced a detailed permafrost dataset from an 1800 km airborne electromagnetic survey conducted in the Yukon Flats, Alaska. Similarly, Parsekian et al. (2013) made surface nuclear magnetic resonance imaging measurements on thermokarst lakes and terrestrial permafrost in Alaska to detect and delineate taliks. The results from recent laboratory tests of saturated or unsaturated soil freezing (e.g., Watanabe et al., 2011; Mohammed et al., 2014) can also be employed to assess the performance of cold regions water flow and heat transport models. We expect similar comprehensive datasets will continue to emerge in the coming years that, coupled with the increased complexity in cold regions hydrogeological modeling (Painter et al., 2013) and increased computing capabilities (Karra et al., 2014), may form the basis to begin to better assess the fidelity of these state-of-the-art models to laboratory and field-scale physical processes.

### 7.3. Translating climate model output to subsurface model boundary conditions

The majority of the climate change impact studies presented in this review that have included the effects of heat advection have assumed a

linear increase in surface temperature due to climate change. However, a linear trend does not adhere to the projections produced by the IPCC, particularly for the higher emission scenarios or representative concentration pathways (Meehl et al., 2007; Kurylyk and MacQuarrie, 2014). Because of the complexity in projected annual and seasonal surface temperature trends, specifying simple functions for the surface temperature boundary condition may not be appropriate. In general, a preferred approach would be to simulate the subsurface thermal influence of future atmospheric climate change by driving groundwater flow and energy transport models with subannual (e.g., daily, weekly, or monthly) global climate model output.

GCMs are typically run on a coarse grid, and thus the results must be downscaled to obtain local-scale climate projections (Step 1b, Fig. 8b). This downscaling can be accomplished through statistical downscaling functions or models (e.g., Wilby and Dawson, 2013). Statistical downscaling functions can be obtained by running the GCM for a reference period, developing relationships/corrections based on the observed meteorological data and the GCM results for that period, and applying those corrections to future period GCM projections (Jeong et al., 2012). Alternatively, higher resolution regional climate models (RCMs), which are driven at the boundaries by GCMs, can be employed to dynamically downscale the GCM results (Wood et al., 2004). Because RCMs often introduce biases, additional debiasing should be performed on the raw RCM output (Bordoy and Burlando, 2013).

Another difficulty in assessing the impacts of climate change to subsurface environments is that subsurface thermal and hydraulic processes are driven by surface conditions (e.g., infiltration and surface temperature), rather than lower atmosphere conditions produced by GCMs (e.g., air temperature and precipitation). Snowpack insulates the ground surface from cold air temperatures during the winter months (Goodrich, 1982b; Zhang, 2005). Thus, the reduction in the thickness and duration of winter snowpack produced by rising air temperatures may decouple decadal surface and air temperature trends (Mann and Schmidt, 2003; Stieglitz et al., 2003; Mellander et al., 2007; Kurylyk et al., 2013). One approach to translate the meteorological changes to surface changes is to utilize the climate scenarios to drive surface models and apply the output

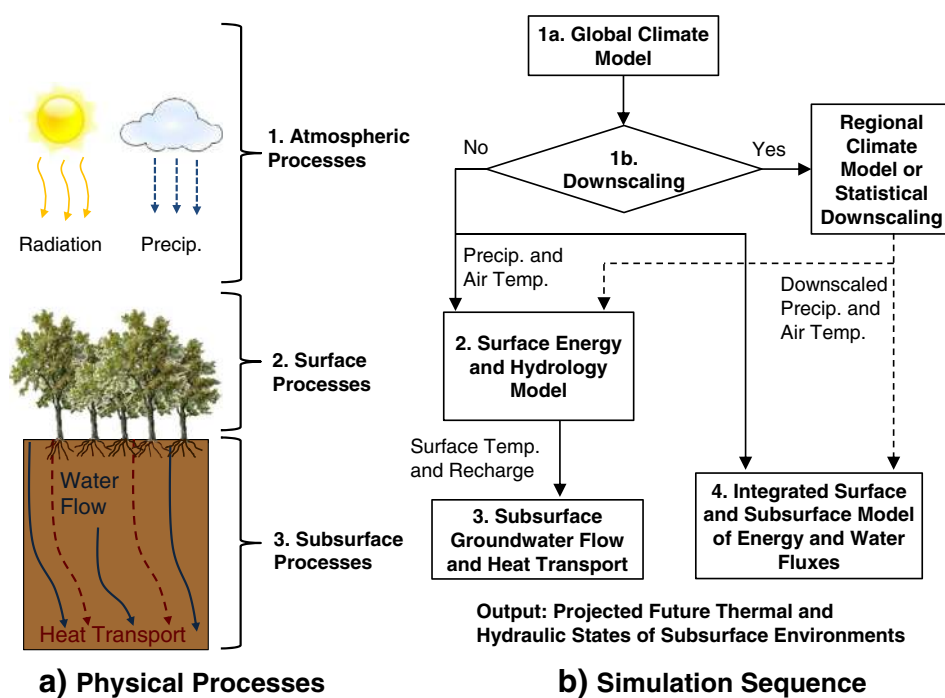


**Fig. 8.** (a) The atmospheric and surface processes that control shallow subsurface thermal regimes and (b) the flowchart for linking atmospheric climate models (Step 1), surface hydrology and energy models (Step 2), and subsurface groundwater flow and heat transport models (Step 3) to reproduce these physical processes. Alternatively, Steps 2 and 3 can be combined in an integrated model capable of simulating surface and subsurface water and energy fluxes (Step 4).

from the surface models as boundary conditions to a groundwater flow and energy transport model (Step 2, Fig. 8b). For example, GCM projections can be utilized to drive a surface heat flux model capable of simulating complex snowpack dynamics (Kurylyk et al., 2013). The ground surface temperature derived from the surficial model can then be applied to form the surface thermal boundary condition for a groundwater flow and heat transport model (Kurylyk et al., 2014a, Step 3, Fig. 8b). Additionally, most of the studies considered in this review ignore the effects of potential increases in advective heat transport due to climate change-induced increases in precipitation and groundwater recharge. Changes to the timing and magnitude of groundwater recharge (Allen et al., 2010; Crosbie et al., 2011; Kurylyk and MacQuarrie, 2013) and subsurface advective heat transport, could be simulated by specifying a climate-controlled groundwater recharge boundary condition obtained by driving a surface hydrological model with the downscaled climate data. The surface thermal and hydrological processes can both be simulated in the same soil vegetation atmosphere transfer model (Step 2, Fig. 8).

Rather than employing an additional surface model, the downscaled climate projections could alternatively be employed to drive integrated models that consider both surface and subsurface thermal processes (e.g., HydroGeoSphere or GEOTop 2.0). This approach (Step 4, Fig. 8b) is preferred to linking surface and subsurface models, although, to our knowledge, no such methodology has yet been employed to simulate the subsurface thermal impact of future climate change in hydrogeologically active environments. In general, most of the studies listed previously have not properly translated GCM projections into appropriate boundary conditions for subsurface models. As climate change science is becoming increasingly multi-disciplinary, progress should be made towards better integration of GCM simulations with surface and subsurface models (Fig. 8).

#### 7.4. Advancing future research in non-permafrost regions

Hydrogeologists have conducted little research on the thermal response of groundwater to future climate change for latitudes and altitudes below the permafrost zone. Even at lower latitudes and altitudes, there will likely be significant changes to surface processes, including increased growing seasons, shifted snowmelt timing, reduced surface albedo and insulation properties due to a reduction in the snow-covered period, altered precipitation regimes, and increased air temperatures. These processes will have an impact on the timing, magnitude, and temperature of groundwater discharge to streams and rivers and could negatively impact groundwater-sourced ecosystems as demonstrated by Kurylyk et al. (2014a). For example, many biological studies have acknowledged the importance of cool groundwater discharge for providing ecological thermal refugia in rivers (e.g., Hynes, 1983; Brunke and Gonser, 1997; Power et al., 1999; Breau et al., 2011; Nichols et al., 2013), and these thermal refugia may be threatened by rising groundwater discharge temperature. Most of the few existing numerical or analytical studies of climate change impacts on groundwater temperature in non-permafrost regions (Taylor and Stefan, 2009; Gunawardhana and Kazama, 2011; Gunawardhana et al., 2011; Kurylyk and MacQuarrie, 2014) have assumed that groundwater flow and heat transport were constrained to one-dimension. These studies have not investigated the thermal impacts of climate change on hydrogeologically complex local and regional scale groundwater systems that can be ecologically important. There is an acknowledged dearth of quantitative hydrogeology studies examining the influence of climate change on groundwater temperature and flow rates and the resultant impacts on riverine and lacustrine thermal regimes (Mayer, 2012; Kanno et al., 2014). Additional studies of this nature would significantly add to our current understanding of the sensitivity of groundwater dependent ecosystems to climate change.

In summary, emerging comprehensive field datasets and powerful hydrogeological numerical models are enhancing our understanding of climate change impacts on subsurface thermal regimes

in cold and temperate regions. Such knowledge provides a greater understanding of the interrelationships between climate change and permafrost degradation, the sensitivity of cold regions infrastructure to climate warming, the potential changes to surface and subsurface hydrological conditions in cold regions, and the deleterious effect of warming groundwater on ecosystems relying on cold groundwater discharge. Despite the recent advancements made in this field, there are still many opportunities for improving our understanding of the relationship between atmospheric climate change and subsurface temperatures. These opportunities include considering advective heat transport in large-scale permafrost degradation studies, comparing cold regions model simulations to field data, linking climate model simulations to surface and subsurface water flow and energy transport models, and conducting related studies for latitudes and altitudes below the permafrost zone.

#### Acknowledgments

We thank Editor Joan Florsheim and two anonymous reviewers for their helpful comments. B.L. Kurylyk was funded by Natural Sciences and Engineering Research Council of Canada postgraduate scholarships (Julie Payette and CGSD3), the Canadian Water Resources Association Dillon Scholarship, and an O'Brien Fellowship.

#### References

- Aldrich, H.P., Paynter, H.M., 1953. *Analytical Studies of Freezing and Thawing in Soils*. U.S. Army Corps Engineers Arctic Construction and Frost Effects Laboratory, Boston, Massachusetts.
- Alexander, M.D., MacQuarrie, K.T.B., Caissie, D., Butler, K.E., 2003. The thermal regime of shallow groundwater and a small Atlantic salmon stream bordering a clearcut with a forested streamside buffer. Annual Conference of the Canadian Society for Civil Engineering. CSCE, Montreal, Quebec, pp. 1899–1908.
- Allen, D.M., Cannon, A.J., Toews, M.W., Scibek, J., 2010. Variability in simulated recharge using different GCMs. *Water Resour. Res.* 46, W00F03.
- Andersland, O.B., Anderson, D.M., 1978. *Geotechnical Engineering for Cold Regions*. McGraw-Hill, New York (384 pp.).
- Andersland, O.B., Ladanyi, B., 1994. *An Introduction to Frozen Ground Engineering*. Chapman & Hall, New York (352 pp.).
- Anderson, M., 2005. Heat as a ground water tracer. *Ground Water* 43 (6), 951–968.
- Anisimov, O.A., Reneva, S., 2006. Permafrost and changing climate: the Russian perspective. *Ambio* 35 (4), 169–175.
- Anisimov, O.A., Shiklomanov, N.I., Nelson, F.E., 2002. Variability of seasonal thaw depth in permafrost regions: a stochastic modeling approach. *Ecol. Model.* 153 (3), 217–227.
- Balland, V., Bhatti, J., Errington, R., Castonguay, M., Arp, P.A., 2006. Modeling snowpack and soil temperature and moisture conditions in a jack pine, black spruce and aspen forest stand in central Saskatchewan (BOREAS SSA). *Can. J. Soil Sci.* 86 (2), 203–217.
- Barlow, J.R.B., Coupe, R.H., 2012. Groundwater and surface-water exchange and resulting nitrate dynamics in the Bogue Phalia Basin in northwestern Mississippi. *J. Environ. Qual.* 41 (1), 155–169.
- Barnhart, C.J., Nimmo, F., Travis, B.J., 2010. Martian post-impact hydrothermal systems incorporating freezing. *Icarus* 208 (1), 101–117.
- Bear, J., 1972. *Dynamics of Fluids in Porous Media*. American Elsevier Publishing Company, Inc., New York, NY (784 pp.).
- Beltrami, H., Chapman, D.S., Archambault, S., Bergeron, Y., 1995. Reconstruction of high resolution ground temperature histories combining dendrochronological and geothermal data. *Earth Planet. Sci. Lett.* 136 (3–4), 437–445.
- Bense, V., Kooi, H., 2004. Temporal and spatial variations of shallow subsurface temperature as a record of lateral variations in groundwater flow. *J. Geophys. Res. Solid Earth* 109 (B4), 1–13.
- Bense, V.F., Ferguson, G., Kooi, H., 2009. Evolution of shallow groundwater flow systems in areas of degrading permafrost. *Geophys. Res. Lett.* 36, L22401.
- Bense, V.F., Kooi, H., Ferguson, G., Read, T., 2012. Permafrost degradation as a control on hydrogeological regime shifts in a warming climate. *J. Geophys. Res. Earth Surf.* 117, 03036.
- Bloomfield, J.P., Jackson, C.R., Stuart, M.E., 2013. Changes in groundwater levels, temperature, and quality in the UK over the 20th century: an assessment of evidence of impacts from climate change. *Living With Environmental Change Report*, UK (14 pp., Available at: <http://nora.nerc.ac.uk/503271/>).
- Bodri, L., Cermak, V., 2007. *Borehole Climatology: A New Method on How to Construct Climate*. Elsevier, Amsterdam (352 pp.).
- Bonan, G., 2008. *Ecological Climatology*. Cambridge University Press, United Kingdom (549 pp.).
- Bons, P.D., van Milligen, B.P., Blum, P., 2013. A general unified expression for solute and heat dispersion in homogeneous porous media. *Water Resour. Res.* 49 (10), 6166–6178.

- Bordoy, R., Burlando, P., 2013. Bias correction of regional climate model simulations in a region of complex orography. *J. Appl. Meteorol. Climatol.* 52 (1), 82–101.
- Breau, C., Cunjak, R.A., Peake, S.J., 2011. Behaviour during elevated water temperatures: can physiology explain movement of juvenile Atlantic salmon to cool water? *J. Anim. Ecol.* 80 (4), 844–853.
- Bredehoeft, J.D., Papadopoulos, I.S., 1965. Rates of vertical groundwater movement estimated from the Earth's thermal profile. *Water Resour. Res.* 1 (2), 325–328.
- Bridger, D.W., Allen, D.M., 2010. Heat transport simulations in a heterogeneous aquifer used for aquifer thermal energy storage (ATES). *Can. Geotech. J.* 47 (1), 96–115.
- Bridger, D.W., Allen, D.M., 2014. Influence of geologic layering on heat transport and storage in an aquifer thermal energy storage system. *Hydrogeol. J.* 22 (1), 233–250.
- Briggs, M.A., Voytek, E.B., Day-Lewis, F.D., Rosenberry, D.O., Lane, J.W., 2013. Understanding water column and streambed thermal refugia for endangered mussels in the Delaware River. *Environ. Sci. Technol.* 47 (20), 11423–11431.
- Briggs, M.A., Walvoord, M.A., McKenzie, J.M., Voss, C.I., Day-Lewis, F.D., Lane, J.W., 2014. New permafrost is forming around shrinking Arctic lakes, but will it last? *Geophys. Res. Lett.* 41 (5), 1585–1592.
- Brown, R.J.E., 1970. Permafrost in Canada; Its Influence on Northern Development. University of Toronto Press, Toronto, ON (234 pp.).
- Brunke, M., Gonser, T., 1997. The ecological significance of exchange processes between rivers and groundwater. *Freshwat. Biol.* 37 (1), 1–33.
- Brunner, P., Simmons, C.T., 2012. HydroGeoSphere: a fully integrated, physically based hydrological model. *Groundwater* 2 (50), 170–176.
- Bullard, E.C., 1939. Heat flow in South Africa. *Proc. R. Soc. Lond.* 173 (955), 474–502.
- Bundschuh, J., 1993. Modeling annual variations of spring and groundwater temperatures associated with shallow aquifer systems. *J. Hydrol.* 142 (1–4), 427–444.
- Burow, K.R., Constantz, J., Fujii, R., 2005. Heat as a tracer to estimate dissolved organic carbon flux from a restored wetland. *Ground Water* 43 (4), 545–556.
- Callegary, J.B., Kikuchi, C.P., Koch, J.C., Lilly, M.R., Leake, S.A., 2013. Review: groundwater in Alaska (USA). *Hydrogeol. J.* 21 (1), 25–39.
- Carlsaw, H.S., Jaeger, J.C., 1959. *Conduction of Heat in Solids*. Clarendon Press, Oxford (520 pp.).
- Changwei, X., Gough, W.A., 2013. Simple thaw-freeze algorithm for a multi-layered soil using the Stefan equation, Permafrost and Periglac. *Process.* 24 (3), 252–260.
- Cheng, G., Jin, H., 2013. Permafrost and groundwater on the Qinghai–Tibet plateau. *Hydrogeol. J.* 21 (1), 5–23.
- Cho, S.H., Sunderland, J.E., 1974. Phase-change problems with temperature-dependent thermal-conductivity. *J. Heat Transf. Trans. ASME* 96 (2), 214–217.
- Connon, R.F., Quinton, W.L., Craig, J.R., Hayashi, M., 2014. Changing hydrologic connectivity due to permafrost thaw in the lower Liard Valley, NWT, Canada. *Hydrol. Process.* <http://dx.doi.org/10.1002/hyp.10206> (Published online).
- Constantz, J., 2008. Heat as a tracer to determine streambed water exchanges. *Water Resour. Res.* 44 (4), W00D10.
- Coon, E.T., Berndt, M., Garimella, R., Mouton, J.D., Painter, S., 2012. A flexible and extensible multi-process simulation capability for the terrestrial Arctic. *Proceedings of the 1st International Conference on Frontiers in Computational Physics: Modeling the Earth System*, Boulder, Colorado.
- Crosbie, R.S., Dawes, W.R., Charles, S.P., Mpelasoka, F.S., Aryal, S., Barron, O., Summerell, G.K., 2011. Differences in future recharge estimates due to GCMs, downscaling methods and hydrological models. *Geophys. Res. Lett.* 38, L11406.
- Dall'Amico, M., Endrizzi, S., Gruber, S., Rigon, R., 2011. A robust and energy-conserving model of freezing variably-saturated soil. *Cryosphere* 5 (2), 469–484.
- Davies, M.C.R., Hamza, O., Harris, C., 2001. The effect of rise in mean annual temperature on the stability of rock slopes containing ice-filled discontinuities. *Permafrost. Periglac. Process.* 12 (1), 137–144.
- de Grandpre, I., Fortier, D., Stephani, E., 2012. Degradation of permafrost beneath a road embankment enhanced by heat advected in groundwater. *Can. J. Earth Sci.* 49 (8), 953–962.
- de Vries, D.A., 1987. The theory of heat and moisture transfer in porous media revisited. *Int. J. Heat Mass Transfer* 30 (7), 1343–1350.
- deVries, D.A., 1963. Thermal properties of soils. In: van Dijk, W.R. (Ed.), *Physics of Plant Environment*. North Holland Publishing, Amsterdam, pp. 210–235.
- Diersch, H.G., 2014. *FEFLOW Finite Element Modeling of Flow, Mass and Heat Transport in Porous and Fractured Media*. Springer-Verlag, Berlin (996 pp.).
- Diersch, H.G., Bauer, D., Heidemann, W., Rühaak, W., Schätzl, P., 2011. Finite element modeling of borehole heat exchanger systems. Part 2. Numerical simulation. *Comput. Geosci.* 37 (8), 1136–1147.
- Dobinski, W., 2011. Permafrost. *Earth-Sci. Rev.* 108 (3–4), 158–169.
- Domenico, P.A., Palciauskas, V.V., 1973. Theoretical analysis of forced convective heat transfer in regional ground-water flow. *Geol. Soc. Am. Bull.* 84 (12), 3803–3814.
- Domenico, P.A., Schwartz, F.W., 1990. *Physical and Chemical Hydrogeology*. Wiley, New York (824 pp.).
- Endrizzi, S., Gruber, S., Dall'Amico, M., Rignon, R., 2013. GEOtop 2.0: simulating the combined energy and water balance at and below the land surface accounting for soil freezing, snow cover and terrain effects. *Geosci. Model Dev. Discuss.* 6, 6279–6341.
- Engeler, I., Hendricks-Franssen, H.J., Müller, R., Stauffer, F., 2011. The importance of coupled modeling of variably saturated groundwater flow-heat transport for assessing river-aquifer interactions. *J. Hydrol.* 397 (3–4), 295–305.
- Etzelmüller, B., Schuler, T.V., Isaksen, K., Christiansen, H.H., Farbrøt, H., Benestad, R., 2011. Modeling the temperature evolution of Svalbard permafrost during the 20th and 21st century. *Cryosphere* 5 (1), 67–79.
- Farouki, O.T., 1981a. The thermal properties of soils in cold regions. *Cold Reg. Sci. Technol.* 5 (1), 67–75.
- Farouki, O.T., 1981b. *Thermal Properties of Soils: CRREL Monograph 81-1*. United States Army Corps of Engineers, Cold Regions Research and Engineering Laboratory, Hanover, New Hampshire (136 pp.).
- Ferguson, G., 2007. Heterogeneity and thermal modeling of ground water. *Ground Water* 45 (4), 485–490.
- Ferguson, G., Woodbury, A.D., 2005. The effects of climatic variability on estimates of recharge from temperature profiles. *Ground Water* 43 (6), 837–842.
- Ferguson, G., Woodbury, A.D., 2007. Urban heat island in the subsurface. *Geophys. Res. Lett.* 34 (23), L23713.
- Ferguson, G., Beltrami, H., Woodbury, A.D., 2006. Perturbation of ground surface temperature reconstructions by groundwater flow? *Geophys. Res. Lett.* 33 (13), L13708.
- Fetter, C.W., 1993. *Contaminant Hydrogeology*. Maxwell Macmillan Canada, Toronto, Ontario (500 pp.).
- Figura, S., Livingstone, D.M., Hoehn, E., Kipfer, R., 2011. Regime shift in groundwater temperature triggered by Arctic oscillation. *Geophys. Res. Lett.* 38 (23), L23401.
- Fischer, L., Kääh, A., Huggel, C., Noetzi, J., 2006. Geology, glacier retreat and permafrost degradation as controlling factors of slope instabilities in a high-mountain rock wall: the Monte Rosa east face. *Nat. Hazards Earth Syst. Sci.* 6 (5), 761–772.
- Flerchinger, G.N., Saxton, K.E., 1989. Simultaneous heat and water model of a freezing snow-residue-soil system. I. Theory and development. *Trans. ASAE* 32 (2), 565–571.
- Forster, C., Smith, L., 1989. The influence of groundwater-flow on thermal regimes in mountainous terrain—a model study. *J. Geophys. Res.* 94 (B7), 9439–9451.
- Fourier, J., 1822. *Theorie analytique de la chaleur (The Analytic Theory of Heat)*. Firmin Didot Père et Fils, Paris.
- Frampton, A., Painter, S.L., Lyon, S.W., Destouni, G., 2011. Non-isothermal, three-phase simulations of near-surface flows in a model permafrost system under seasonal variability and climate change. *J. Hydrol.* 403 (3–4), 352–359.
- Frampton, A., Painter, S.L., Destouni, G., 2013. Permafrost degradation and subsurface-flow changes caused by surface warming trends. *Hydrogeol. J.* 21 (1), 271–280.
- Freitag, D.R., McFadden, T.T., 1997. *Introduction to Cold Regions Engineering*. ASCE Press, New York (738 pp.).
- French, H.M., 2007. *The Periglacial Environment*, 3rd ed. John Wiley & Sons Ltd, Sussex, England (480 pp.).
- Ge, S., McKenzie, J.M., Voss, C.I., Wu, Q., 2011. Exchange of groundwater and surface-water mediated by permafrost response to seasonal and long term air temperature variation. *Geophys. Res. Lett.* 38 (14), L14402.
- Goderniaux, P., Brouyère, S., Fowler, H.J., Blenkinsop, S., Therrien, R., Orban, P., Dassargues, A., 2009. Large scale surface-subsurface hydrological model to assess climate change impacts on groundwater reserves. *J. Hydrol.* 373 (1–2), 122–138.
- Gold, L.W., Lachenbruch, A.H., 1973. Thermal conditions in permafrost—a review of North American literature. *North American Contribution to the Second International Conference on Permafrost*. National Academy of Science, Washington DC, pp. 3–25.
- Goodrich, L.E., 1982a. *An Introductory Review of Numerical Methods for Ground Thermal Regime Calculations*. Division of Building Research, National Research Council of Canada, Ottawa, Ontario (32 pp.).
- Goodrich, L.E., 1982b. The influence of snow cover on the ground thermal regime. *Can. Geotech. J.* 19 (4), 421–432.
- Gordon, R.P., Lutz, L.K., Briggs, M.A., McKenzie, J.M., 2012. Automated calculation of vertical pore-water flux from field temperature time series using the VFLUX method and computer program. *J. Hydrol.* 420–421, 142–158.
- Gouttevin, I., Krinner, G., Clais, P., Polcher, J., Legout, C., 2012. Multi-scale validation of a new soil freezing scheme for a land-surface model with physically-based hydrology. *Cryosphere* 6 (2), 407–430.
- Green, T.R., Taniguchi, M., Kooi, H., Gurdak, J.J., Allen, D.M., Hiscock, K.M., Treidel, H., Aureli, A., 2011. Beneath the surface of global change: impacts of climate change on groundwater. *J. Hydrol.* 405 (3–4), 532–560.
- Grenier, C., Régnier, D., Mouche, E., Benabderrahmane, H., Costard, F., Davy, P., 2013. Impact of permafrost development on groundwater flow patterns: a numerical study considering freezing cycles on a two-dimensional vertical cut through a generic river-plain system. *Hydrogeol. J.* 21 (1), 257–270.
- Grimm, R.E., Painter, S.L., 2009. On the secular evolution of groundwater on Mars. *Geophys. Res. Lett.* 36 (24), L24803.
- Gruber, S., Haeberli, W., 2007. Permafrost in steep bedrock slopes and its temperature-related destabilization following climate change. *J. Geophys. Res. Earth Surf.* 112 (F2), F02S18.
- Gunawardhana, L.N., Kazama, S., 2011. Climate change impacts on groundwater temperature change in the Sendai plain, Japan. *Hydrol. Process.* 25 (17), 2665–2678.
- Gunawardhana, L.N., Kazama, S., 2012. Statistical and numerical analyses of the influence of climate variability on aquifer water levels and groundwater temperatures: the impacts of climate change on aquifer thermal regimes. *Glob. Planet. Chang.* 86–87, 66–78.
- Gunawardhana, L.N., Kazama, S., Kawagoe, S., 2011. Impact of urbanization and climate change on aquifer thermal regimes. *Water Resour. Manag.* 25 (13), 3247–3276.
- Guo, D., Wang, H., Li, D., 2012. A projection of permafrost degradation on the Tibetan Plateau during the 21st century. *J. Geophys. Res. Atmos.* 117, D05106.
- Guymon, G.L., Luthin, J.N., 1974. A coupled heat and moisture transport model for Arctic soils. *Water Resour. Res.* 10 (5), 995–1001.
- Hähnlein, S., Bayer, P., Ferguson, G., Blum, P., 2013. Sustainability and policy for the thermal use of shallow geothermal energy. *Energy Policy* 59, 914–925.
- Haldorsen, S., Heim, M., Dale, B., Landvik, J.Y., van der Ploeg, M., Leijnse, A., Salvijsen, O., Hagen, J.O., Banks, D., 2010. Sensitivity to long-term climate change of subpermafrost groundwater systems in Svalbard. *Quat. Res.* 73 (2), 393–402.
- Hansson, K., Simunek, J., Mizoguchi, M., Lundin, L.C., van Genuchten, M.T., 2004. Water flow and heat transport in frozen soil: numerical solution and freeze-thaw applications. *Vadose Zone J.* 3 (2), 693–704.
- Harden, J.W., Koven, C.D., Ping, C., Hugelius, G., McGuire, A.D., Camill, P., Jorgenson, T., Kuhry, P., Michaelson, G.J., O'Donnell, J.A., Schuur, E.A.G., Tarnocai, C., Johnson, K., Grosse, G., 2012. Field information links permafrost carbon to physical vulnerabilities of thawing. *Geophys. Res. Lett.* 39, L15704.

- Harlan, R.L., 1973. Analysis of coupled heat-fluid transport in partially frozen soil. *Water Resour. Res.* 9 (5), 1314–1323.
- Harlan, R.L., Nixon, J.F., 1978. Chapter 3: ground thermal regime. *Geotechnical Engineering for Cold Regions*. McGraw-Hill Inc., USA, pp. 103–163.
- Harris, C., Arenson, L.U., Christiansen, H.H., Etzelmüller, B., Frauenfelder, R., Gruber, S., Haeberli, W., Hauck, C., Hoelzle, M., Humlum, O., Isaksen, K., Kääb, A., Kern-Lütsch, M.A., Lehning, M., Matsuoka, N., Murtun, J.B., Noežli, J., Phillips, M., Ross, N., Seppala, M., Springman, S.M., Mühl, D.V., 2009. Permafrost and climate in Europe: monitoring and modelling thermal, geomorphological and geotechnical responses. *Earth Sci. Rev.* 92 (3–4), 117–171.
- Hasler, A., Gruber, S., Font, M., Dubois, A., 2011. Advective heat transport in frozen rock clefts: conceptual model, laboratory experiments and numerical simulation. *Permafrost. Periglac. Process.* 22 (4), 378–389.
- Hatch, C.E., Fisher, A.T., Revenaugh, J.S., Constantz, J., Ruelh, C., 2006. Quantifying surface water–groundwater interactions using time series analysis of streambed thermal records: method development. *Water Resour. Res.* 42 (10), W10410.
- Hayashi, M., Rosenberry, D.O., 2001. Effects of ground water exchange on the hydrology and ecology of surface water. *Ground Water* 40 (3), 309–316.
- Hayashi, M., Goeller, N., Quinton, W.L., Wright, N., 2007. A simple heat-conduction method for simulating the frost–table depth in hydrological models. *Hydrol. Process.* 21 (19), 2610–2622.
- Healy, R.W., Ronan, A.D., 1996. Documentation of computer program VS2Dh for simulation of energy transport in variably saturated porous media; modifications of the US Geological Survey's computer program VS2DT. U.S. Geological Survey Water- Investigations Report. Denver, CO (36 pp.).
- Heginbottom, J.A., Brown, J., Melnikov, E.S., Ferrians Jr., O.J., 1993. Circum-arctic map of permafrost and ground ice conditions. *Permafrost: Proceedings of the Sixth International Conference*, China. South China Univ. Technol. Press, pp. 1132–1136.
- Hinkel, K.M., 1997. Estimating seasonal values of thermal diffusivity in thawed and frozen soils using temperature time series. *Cold Reg. Sci. Technol.* 26 (1), 1–15.
- Hinkel, K.M., Nicholas, J.R.J., 1995. Active layer thaw rate at a boreal forest site in central Alaska, USA. *Arct. Alp. Res.* 27 (1), 72–80.
- Hinzman, L., Bettez, N., Bolton, W., Chapin, F., Dyrgerov, M., Fastie, C., Griffith, B., Hollister, R., Hope, A., Huntington, H., Jensen, A., Jia, G., Jorgenson, T., Kane, D., Klein, D., Kofinas, G., Lynch, A., Lloyd, A., McGuire, A., Nelson, F., Oechel, W., Osterkamp, T., Racine, C., Romanovsky, V., Stone, R., Stow, D., Sturm, M., Tweedie, C., Vourlitis, G., Walker, M., Walker, D., Webber, P., Welker, J., Winker, K., Yoshikawa, K., 2005. Evidence and implications of recent climate change in northern Alaska and other Arctic regions. *Clim. Chang.* 72 (3), 251–298.
- Hipp, T., Etzelmüller, B., Farbrøt, H., Schuler, T.V., Westermann, S., 2012. Modelling borehole temperatures in Southern Norway – insights into permafrost dynamics during the 20th and 21st century. *Cryosphere* 6 (3), 553–571.
- Hsieh, P., Wingle, W., Healy, R.H., 2000. VS2DI – a graphical software package for simulating fluid flow and solute or energy transport in variably saturated porous media. U.S. Geological Survey Water-Resources Investigations Report 9. Lakewood, CO (20 pp.).
- Hynes, H.B.N., 1983. Groundwater and stream ecology. *Hydrobiologia* 100 (1), 93–99.
- Ingebritsen, S.E., Sanford, W.E., Neuzil, C.E., 2006. *Groundwater in Geologic Processes*, 2nd ed. Cambridge University Press, New York (564 pp.).
- Ippisch, D.O., 2001. Coupled Transport in Natural Porous Media (Doctor of Natural Sciences Dissertation) University of Heidelberg, Heidelberg, Germany (145 pp.).
- Ireson, A.M., van der Kamp, G., Ferguson, G., Nachshon, U., Wheatler, H.S., 2013. Hydrogeological processes in seasonally frozen northern latitudes: understanding, gaps and challenges. *Hydrogeol. J.* 21 (1), 53–66.
- Jafarov, E.E., Marchenko, S.S., Romanovsky, V.E., 2012. Numerical modeling of permafrost dynamics in Alaska using a high spatial resolution dataset. *Cryosphere* 6 (3), 613–624.
- Jame, Y.W., Norum, D.I., 1980. Heat and mass-transfer in a freezing unsaturated porous-medium. *Water Resour. Res.* 16 (4), 811–819.
- Jeong, D.I., St-Hilaire, A., Ourarda, T.B.M.J., Gachon, P., 2012. A multivariate multi-site statistical downscaling model for daily maximum and minimum temperatures. *Clim. Res.* 54, 129–148.
- Jiang, Y., Zhuang, Q., Schaphoff, S., Sitch, S., Sokolov, A., Kicklighter, D., Melillo, J., 2012a. Uncertainty analysis of vegetation distribution in the northern high latitudes during the 21st century with a dynamic vegetation model. *Ecol. Evol.* 2 (3), 593–614.
- Jiang, Y., Zhuang, Q., O'Donnell, J.A., 2012b. Modeling thermal dynamics of active layer soils and near-surface permafrost using a fully coupled water and heat transport model. *J. Geophys. Res. Atmos.* 117, D11110.
- Jin, H., Zhao, L., Wang, S., Jin, R., 2006. Thermal regimes and degradation modes of permafrost along the Qinghai–Tibet Highway. *Sci. China. Ser. D Earth Sci.* 49 (11), 1170–1183.
- Jones, C.E., Kielland, K., Hinzman, L.D., 2013. Modeling groundwater upwelling as a control on river ice thickness. *Proceedings of the 19th International Northern Research Basins Symposium and Workshop*, Southcentral Alaska, USA, pp. 107–115.
- Jorgenson, M.T., Racine, C.H., Walters, J.C., Osterkamp, T.E., 2001. Permafrost degradation and ecological changes associated with a warming climate in central Alaska. *Clim. Chang.* 48 (4), 551–579.
- Jorgenson, M.T., Romanovsky, V., Harden, J., Shur, Y., O'Donnell, J., Schuur, E.A.G., Kanevskiy, M., Marchenko, S., 2010. Resilience and vulnerability of permafrost to climate change. *Can. J. For. Res.* 40 (7), 1219–1236.
- Jumikis, A.R., 1966. *Thermal Soil Mechanics*. Rutgers University Press, New Brunswick, N.J. (267 pp.).
- Kahimba, F.C., Ranjan, R.S., Mann, D.D., 2009. Modeling soil temperature, frost depth, and soil moisture redistribution in seasonally frozen agricultural soils. *Appl. Eng. Agric.* 25 (6), 871–882.
- Kane, D.L., Hinzman, L.D., Zarling, J.P., 1991. Thermal response of the active layer to climatic warming in a permafrost environment. *Cold Reg. Sci. Technol.* 19 (2), 111–122.
- Kane, D.L., Hinkel, K.M., Goering, D.J., Hinzman, L.D., Outcalt, S.I., 2001. Non-conductive heat transfer associated with frozen soils. *Glob. Planet. Chang.* 29 (3–4), 275–292.
- Kane, D.L., Yoshikawa, K., McNamara, J.P., 2013. Regional groundwater flow in an area mapped as continuous permafrost, NE Alaska (USA). *Hydrogeol. J.* 21 (1), 41–52.
- Kanno, Y., Vokoun, J.C., Letcher, B.H., 2014. Paired stream–air temperature measurements reveal fine-scale thermal heterogeneity within headwater brook trout stream networks. *River Res. Appl.* <http://dx.doi.org/10.1002/rra.2677> (Published online).
- Karra, S., Painter, S.L., Lichtner, P.C., 2014. Three-phase numerical model for subsurface hydrology in permafrost-affected regions. *Cryosphere Discuss.* 8, 149–185.
- Kay, B.D., Fukuda, M., Izuta, H., Sheppard, M.I., 1981. The importance of water migration in the measurement of the thermal conductivity of unsaturated frozen soils. *Cold Reg. Sci. Technol.* 5 (2), 95–106.
- Kelvin, W., 1861. On the reduction of observations of underground temperature. *Trans. R. Soc. Edinb.* 22, 405–427.
- Kettridge, N., Baird, A., 2008. Modelling soil temperatures in northern peatlands. *Eur. J. Soil Sci.* 59 (2), 327–338.
- Klene, A.E., Nelson, F.E., Shiklomanov, N.I., Hinkel, K.M., 2001. The n factor in natural landscapes: variability of air and soil-surface temperatures, Kuparuk River Basin, Alaska, USA. *Arct. Antarct. Alp. Res.* 33 (2), 140–148.
- Kløve, B., et al., 2011. Groundwater dependent ecosystems. Part I. Hydroecological status and trends. *Environ. Sci. Policy* 14 (7), 770–781.
- Koo, M., Kim, Y., 2008. Modeling of water flow and heat transport in the vadose zone: numerical demonstration of variability of local groundwater recharge in response to monsoon rainfall in Korea. *Geosci. J.* 12 (2), 123–137.
- Koopmans, R.W.R., Miller, R.D., 1966. Soil freezing and soil water characteristic curves. *Soil Sci. Soc. Am. Proc.* 30 (6), 680–685.
- Krzewinski, T.G., Tart, R.G. (Eds.), 1985. *Technical council on cold regions engineering, 1985. Thermal Design Considerations in Frozen Ground Engineering: A State of the Practice Report* ASCE, New York, N.Y. (277 pp.).
- Kukkonen, I.T., Clauser, C., 1994. Simulation of heat-transfer at the Kola deep-hole site – implications for advection, heat refraction and paleoclimatic effects. *Geophys. J. Int.* 116 (2), 409–420.
- Kukkonen, I.T., Cermák, V., Safanda, J., 1994. Subsurface temperature–depth profiles, anomalies due to climatic ground surface temperature changes or groundwater flow effects. *Glob. Planet. Chang.* 9 (3–4), 221–232.
- Kumar, R.R., Ramana, D.V., Singh, R.N., 2012. Modelling near subsurface temperature with mixed type boundary condition for transient air temperature and vertical groundwater flow. *J. Earth Syst. Sci.* 121 (5), 1177–1184.
- Kurylyk, B.L., MacQuarrie, K.T.B., 2013. The uncertainty associated with estimating future groundwater recharge: a summary of recent research and an example from a small unconfined aquifer in a northern climate. *J. Hydrol.* 492 (7), 244–253.
- Kurylyk, B.L., MacQuarrie, K.T.B., 2014. A new analytical solution for assessing projected climate change impacts on subsurface temperature. *Hydrol. Process.* 28 (7), 3161–3172.
- Kurylyk, B.L., Watanabe, K., 2013. The mathematical representation of freezing and thawing processes in variably-saturated, non-deformable soils. *Adv. Water Resour.* 60, 160–177.
- Kurylyk, B.L., Bourque, C.P.A., MacQuarrie, K.T.B., 2013. Potential surface temperature and shallow groundwater temperature response to climate change: an example from a small forested catchment in east-central New Brunswick (Canada). *Hydrol. Earth Syst. Sci.* 17, 2701–2716.
- Kurylyk, B.L., MacQuarrie, K.T.B., Voss, C.I., 2014a. Climate change impacts on the temperature and magnitude of groundwater discharge from shallow, unconfined aquifers. *Water Resour. Res.* 50 (4), 3253–3274.
- Kurylyk, B.L., McKenzie, J.M., MacQuarrie, K.T.B., Voss, C.I., 2014b. Analytical solutions for benchmarking cold regions subsurface water flow and energy transport models: one dimensional soil thaw with conduction and advection. *Adv. Water Resour.* 70, 172–184.
- Lapham, W.W., 1989. Use of temperature profiles beneath streams to determine rates of groundwater flow and vertical hydraulic conductivity. U.S. Geological Survey Water Supply Paper USGS, Denver, CO (44 pp.).
- Lawrence, D.M., Slater, A.G., Swenson, S.C., 2012. Simulation of present-day and future permafrost and seasonally frozen ground conditions in CCSM4. *J. Clim.* 25 (7), 2207–2225.
- Lesperance, M., Smerdon, J.E., Beltrami, H., 2010. Propagation of linear surface air temperature trends into the terrestrial subsurface. *J. Geophys. Res. Atmos.* 115 (21), D21115.
- Li, Q., Sun, S., Xue, Y., 2010. Analyses and development of a hierarchy of frozen soil models for cold region study. *J. Geophys. Res. Atmos.* 115 (D3), D03107.
- Liu, Z., Yu, X., 2011. Coupled thermo-hydro-mechanical model for porous materials under frost action: theory and implementation. *Acta Geotech.* 6 (2), 51–65.
- Lock, G.S.H., Gunderson, J.R., Quon, D., Donnelly, J.K., 1969. A study of one-dimensional ice formation with particular reference to periodic growth and decay. *Int. J. Heat Mass Transfer* 12 (11), 1343–1352.
- Lu, N., Ge, S., 1996. Effect of horizontal heat and fluid flow on the vertical temperature distribution in a semiconfining layer. *Water Resour. Res.* 32 (5), 1449–1453.
- Luce, C.H., Tonina, D., Gariglio, F., Applebee, R., 2013. Solutions for the diurnally forced advection–diffusion equation to estimate bulk fluid velocity and diffusivity in streambeds from temperature time series. *Water Resour. Res.* 49 (1), 488–506.
- Lunardini, V.J., 1981. *Heat Transfer in Cold Climates*. Van Nostrand Reinhold Co., New York (731 pp.).
- Lunardini, V.J., 1985. Section 8: analytical methods for ground thermal regime calculations. *Technical Council on Cold Regions Engineering Monograph: Thermal Design Considerations in Frozen Ground Engineering*. American Society of Civil Engineers, New York, NY, pp. 204–257.
- Lunardini, V.J., 1991. *Heat Transfer with Freezing and Thawing*. Elsevier Science Pub. Co., New York, NY (437 pp.).

- Lunardini, V.J., 1998. Effect of convective heat transfer on thawing of frozen soil. *Permafrost, Seventh International Conference*. Laval University, Quebec, Canada, pp. 689–695.
- Luo, L.F., Robock, A., Vinnikov, K.Y., Schlosser, C.A., Slater, A.G., Boone, A., Braden, H., Cox, P., de Rosnay, P., Dickinson, R.E., Dai, Y.J., Duan, Q.Y., Etchevers, P., Henderson-Sellers, A., Gedney, N., Gusev, Y.M., Habets, F., Kim, J.W., Kowalczyk, E., Mitchell, K., Nasonova, O.N., Noilhan, J., Pitman, A.J., Schaake, J., Shmakin, A.B., Smirnova, T.G., Wetzell, P., Xue, Y.K., Yang, Z.L., Zeng, Q.C., 2003. Effects of frozen soil on soil temperature, spring infiltration, and runoff: results from the PILPS 2(d) experiment at Valdai, Russia. *J. Hydrometeorol.* 4 (2), 334–351.
- Lyon, S.W., Destouni, G., Giesler, R., Humborg, C., Morth, M., Seibert, J., Karlsson, J., Troch, P.A., 2009. Estimation of permafrost thawing rates in a sub-arctic catchment using recession flow analysis. *Hydrol. Earth Syst. Sci.* 13 (5), 595–604.
- Mann, M., Schmidt, G., 2003. Ground vs. surface air temperature trends: implications for borehole surface temperature reconstructions. *Geophys. Res. Lett.* 30 (12), 1607.
- Mareschal, J., Beltrami, H., 1992. Evidences for recent warming from perturbed geothermal gradients: examples from eastern Canada. *Clim. Dyn.* 6 (3–4), 135–143.
- Markle, J.M., Schincariol, R.A., 2007. Thermal plume transport from sand and gravel pits – potential thermal impacts on cool water streams. *J. Hydrol.* 338 (3–4), 174–195.
- Markle, J.M., Schincariol, R.A., Sass, J.H., Molson, J.W., 2006. Characterizing the two-dimensional thermal conductivity distribution in a sand and gravel aquifer. *Soil Sci. Soc. Am. J.* 70 (4), 1281–1294.
- Marshall, S.J., 2012. *The Cryosphere*. Princeton University Press, Princeton, New Jersey (288 pp.).
- Matell, N., Anderson, R.S., Overeem, I., Wobus, C., Urban, F.E., Clow, G.D., 2013. Modeling the subsurface thermal impact of Arctic thaw lakes in a warming climate. *Comput. Geosci.* 53, 69–79.
- Mauro, G., 2004. Observations on permafrost ground thermal regimes from Antarctica and the Italian Alps, and their relevance to global climate change. *Glob. Planet. Chang.* 40 (1–2), 159–167.
- Mayer, T., 2012. Controls of summer stream temperature in the Pacific Northwest. *J. Hydrol.* 475 (19), 323–335.
- McGuire, A.D., Christensen, T.R., Hayes, D., Heroult, A., Euskirchen, E., Kimball, J.S., Koven, C., Laflour, P., Miller, P.A., Oechel, W., Peylin, P., Williams, M., Yi, Y., 2012. An assessment of the carbon balance of Arctic tundra: comparisons among observations, process models, and atmospheric inversions. *Biogeosciences* 9 (8), 3185–3204.
- McKenzie, J.M., Voss, C.I., 2013. Permafrost thaw in a nested groundwater-flow system. *Hydrogeol. J.* 21 (1), 299–316.
- McKenzie, J.M., Siegel, D.I., Rosenberry, D.O., Glaser, P.H., Voss, C.I., 2006. Heat transport in the Red Lake Bog, Glacial Lake Agassiz Peatlands. *Hydrol. Process.* 21 (3), 369–378.
- McKenzie, J.M., Voss, C.I., Siegel, D.I., 2007. Groundwater flow with energy transport and water–ice phase change: numerical simulations, benchmarks, and application to freezing in peat bogs. *Adv. Water Resour.* 30 (4), 966–983.
- Meehl, G.A., Stocker, T.F., Collins, W.D., Friedlingstein, P., Gaye, A.T., Gregory, J.M., Kitoh, A., Knutti, R., Murphy, J.M., Noda, A., Raper, S.C.B., Watterson, I.G., Weaver, A.J., Zhao, Z., 2007. Global climate projections. *Climate Change 2007: the physical science basis*. Contributions of Working Group 1 to the Fourth Assessment Report of the Intergovernmental Panel on Climate Change. Cambridge University Press, Cambridge, UK (pp. SM.10-1–Sm. 10-8).
- Mellander, P., Lofvenius, M.O., Laudon, H., 2007. Climate change impact on snow and soil temperature in boreal Scots pine stands. *Clim. Chang.* 89 (1–2), 179–193.
- Menberg, K., Blum, P., Schafflitz, A., Bayer, P., 2013. Long-term evolution of anthropogenic heat fluxes into a subsurface urban heat island. *Environ. Sci. Technol.* 47 (17), 9747–9755.
- Menberg, K., Blum, P., Kurylyk, B.L., Bayer, P., 2014. Observed groundwater temperature response to recent climate change. *Hydrol. Earth Syst. Sci. Discuss.* 11, 3637–3673.
- Michel, F.A., van Everdingen, R.O., 2006. Changes in hydrogeologic regimes in permafrost regions due to climatic change. *Permafr. Periglac. Process.* 5 (3), 191–195.
- Miller, R.D., 1972. Freezing and heaving of saturated and unsaturated soils. *Highw. Res. Rec.* 393, 1–11.
- Miller, R.D., 1980. Freezing phenomena in soils. *Application of Soil Physics*. Academic Press, New York, New York, pp. 254–299.
- Minsley, B.J., Abraham, J.D., Smith, B.D., Cannia, J.C., Voss, C.I., Jorgenson, M.T., Walvoord, M.A., Wylie, B.K., Anderson, L., Ball, L.B., Deszcz-Pan, M., Wellman, T.P., Ager, T.A., 2012. Airborne electromagnetic imaging of discontinuous permafrost. *Geophys. Res. Lett.* 39, L02503.
- Miyakoshi, A., Uchida, Y., Sakura, Y., Hayashi, T., 2003. Distribution of subsurface temperature in the Kanto Plain, Japan; estimation of regional groundwater flow system and surface warming. *Phys. Chem. Earth* 28 (9–11), 467–475.
- Mizoguchi, M., 1990. *Water, Heat and Salt Transport in Freezing Soil (in Japanese)* (Doctor of Philosophy Dissertation) University of Tokyo, Tokyo, Japan.
- Mohammed, A.A., Schincariol, R.A., Nagare, R.M., Quinton, W.L., 2014. Reproducing field-scale active layer thaw in the lab. *Vadose Zone J.* <http://dx.doi.org/10.2136/vzj2014.01.0008> (Published online).
- Molina-Giraldo, N., Bayer, P., Blum, P., 2011. Evaluating the influence of thermal dispersion on temperature plumes from geothermal systems using analytical solutions. *Int. J. Therm. Sci.* 50 (7), 1223–1231.
- Nelson, F.E., Shiklomanov, N.I., Mueller, G.R., Hinkel, K.M., Walker, D.A., Bockheim, J.G., 1997. Estimating active-layer thickness over a large region: Kuparuk River Basin, Alaska, USA. *Arct. Alp. Res.* 29 (4), 367–378.
- Newman, G., Wilson, G., 1997. Heat and mass transfer in unsaturated soils during freezing. *Can. Geotech. J.* 34 (1), 63–70.
- Nichols, A.L., Willis, A.D., Jeffers, C.A., Deas, M.L., 2013. Water temperature patterns below large groundwater springs: management implications for Coho Salmon in the Shasta River, California. *River Res. Appl.* 30 (4), 442–455.
- Nixon, J.F., 1975. The role of convective heat transport in the thawing of frozen soils. *Can. Geotech. J.* 12, 425–529.
- Nixon, J.F., McRoberts, E.C., 1973. A study of some factors affecting the thawing of frozen soils. *Can. Geotech. J.* 10 (3), 439–452.
- Noetzli, J., Gruber, S., Kohl, T., Salzmann, N., Haeberli, W., 2007. Three-dimensional distribution and evolution of permafrost temperatures in idealized high-mountain topography. *J. Geophys. Res. Earth Surf.* 112, F2.
- Oechel, W.C., Hastings, S.J., Vourlitis, G., Jenkins, M., Riechers, G., Grulke, N., 1993. Recent change of Arctic tundra ecosystems from a net carbon-dioxide sink to a source. *Nature* 361 (6412), 520–523.
- Oke, T.R., 1978. *Boundary Layer Climates*. Methuen and Co., London (435 pp.).
- Overduin, P.P., Kane, D.L., van Loon, W.K.P., 2006. Measuring thermal conductivity in freezing and thawing soil using the soil temperature response to heating. *Cold Reg. Sci. Technol.* 45 (1), 8–22.
- Öz i k, M.N., 1980. *Heat Conduction*. Wiley, New York (687 pp.).
- Painter, S., 2011. Three-phase numerical model of water migration in partially frozen geological media: model formulation, validation, and applications. *Comput. Geosci.* 15 (1), 69–85.
- Painter, S.L., Moulton, J.D., Wilson, C.J., 2013. Modeling challenges for predicting hydrologic response to degrading permafrost. *Hydrogeol. J.* 21 (1), 221–224.
- Pang, Q., Zhao, L., Li, S., Ding, Y., 2012. Active layer thickness variations on the Qinghai–Tibet Plateau under the scenarios of climate change. *Environ. Earth Sci.* 66 (3), 849–857.
- Parsekian, A.D., Grosse, G., Walbrecker, J.O., Müller-Petke, M., Keating, B.K., Liu, L., Jones, B.M., Knight, R., 2013. Detecting unfrozen sediments below thermokarst lakes with surface nuclear magnetic resonance. *Geophys. Res. Lett.* 40 (3), 535–540.
- Parsons, M.L., 1970. Groundwater thermal regime in a glacial complex. *Water Resour. Res.* 6 (6), 1701–1720.
- Power, G., Brown, R.S., Imhof, J.G., 1999. Groundwater and fish – insights from northern North America. *Hydrol. Process.* 13 (3), 401–422.
- Qian, B., Gregorich, E.G., Gameda, S., Hopkins, D.W., Wang, X.L., 2011. Observed soil temperature trends associated with climate change in Canada. *J. Geophys. Res. Atmos.* 116, D02106.
- Quinton, W.L., Baltzer, J.L., 2013. The active-layer hydrology of a peat plateau with thawing permafrost (Scotty Creek, Canada). *Hydrogeol. J.* 21 (1), 201–220.
- Quinton, W.L., Hayashi, M., Chasmer, L.E., 2011. Permafrost–thaw-induced land-cover change in the Canadian subarctic: implications for water resources. *Hydrol. Process.* 25 (1), 152–158.
- Rau, G.C., Anderson, M.S., Acworth, R.I., 2012. Experimental investigation of the thermal dispersivity term and its significance in the heat transport equation for flow in sediments. *Water Resour. Res.* 48 (3), W03511.
- Rau, G.C., Anderson, M.S., McCallum, A.M., Roshan, H., Acworth, R.I., 2014. Heat as a tracer to quantify water flow in near-surface sediments. *Earth-Sci. Rev.* 129, 40–58.
- Reiter, M., 2001. Using precision temperature logs to estimate horizontal and vertical groundwater flow components. *Water Resour. Res.* 37 (3), 663–674.
- Rike, A.G., Schiewer, S., Filler, D.M., 2008. Chapter 5: temperature effects on biodegradation of petroleum contaminants in cold soils. *Bioremediation of Petroleum Hydrocarbons in Cold Regions*. Cambridge University Press, Cambridge, UK, pp. 84–108.
- Riseborough, D., Shiklomanov, N., Etzelmüller, B., Gruber, S., Marchenko, S., 2008. Recent advances in permafrost modelling. *Permafr. Periglac. Process.* 19 (2), 137–156.
- Romanovsky, V., Osterkamp, T., 1997. Thawing of the active layer on the coastal plain of the Alaskan Arctic. *Permafr. Periglac. Process.* 8 (1), 1–22.
- Romanovsky, V.E., Smith, S.L., Christiansen, H.H., 2010. Permafrost thermal state in the polar Northern Hemisphere during the international polar year 2007–2009: a synthesis. *Permafr. Periglac. Process.* 21 (2), 106–116.
- Rouse, W.R., Douglas, M.S.V., Hecky, R.E., Hershey, A.E., Kling, G.W., Lesack, L., Marsh, P., McDonald, M., Nicholson, B.J., Roulet, N.T., Smol, J.P., 1997. Effects of climate change on the freshwaters of Arctic and subarctic North America. *Hydrol. Process.* 11 (8), 873–902.
- Rowland, J.C., Travis, B.J., Wilson, C.J., 2011. The role of advective heat transport in talik development beneath lakes and ponds in discontinuous permafrost. *Geophys. Res. Lett.* 38 (17), L17504.
- Saar, M.O., 2011. Review: geothermal heat as a tracer of large-scale groundwater flow and as a means to determine permeability fields. *Hydrogeol. J.* 19 (1), 31–52.
- Saito, H., Simunek, J., Mohanty, B.P., 2006. Numerical analysis of coupled water, vapor, and heat transport in the vadose zone. *Vadose Zone J.* 5 (2), 784–800.
- Sauty, J.P., Gringarten, A.C., Menjoz, A., 1982. Sensible energy storage in aquifers. 1. Theoretical study. *Water Resour. Res.* 18 (2), 245–252.
- Schaefer, K., Zhang, T., Bruhwiler, L., Barrett, A.P., 2011. Amount and timing of permafrost carbon release in response to climate warming. *Tellus Ser. B Chem. Phys. Meteorol.* 63 (2), 165–180.
- Schindler, D.W., Smol, J.P., 2006. Cumulative effects of climate warming and other human activities on freshwaters of Arctic and subarctic North America. *Ambio* 35 (4), 160–168.
- Serreze, M., Walsh, J., Chapin, F., Osterkamp, T., Dyurgerov, M., Romanovsky, V., Oechel, W., Morison, J., Zhang, T., Barry, R., 2000. Observational evidence of recent change in the northern high-latitude environment. *Clim. Chang.* 46 (1–2), 159–207.
- Sharma, L., Greskowiak, J., Ray, C., Eckert, P., Prommer, H., 2012. Elucidating temperature effects on seasonal variations of biogeochemical turnover rates during riverbank filtration. *J. Hydrol.* 428–429, 104–115.
- Shoop, S., Bigl, S., 1997. Moisture migration during freeze and thaw of unsaturated soils: modeling and large scale experiments. *Cold Reg. Sci. Technol.* 25 (1), 33–45.
- Shur, Y.L., Jorgenson, M.T., 2007. Patterns of permafrost formation and degradation in relation to climate and ecosystems. *Permafr. Periglac. Process.* 18 (1), 7–19.
- Sjöberg, Y., Frampton, A., Lyon, S.W., 2013. Using streamflow characteristics to explore permafrost thawing in northern Swedish catchments. *Hydrogeol. J.* 21 (1), 121–131.

- Smith, L., Chapman, D.S., 1983. On the thermal effects of groundwater flow. 1. Regional scale systems. *J. Geophys. Res.* 88 (1), 593–608.
- Smith, L.C., Sheng, Y., MacDonald, G.M., Hinzmann, L.D., 2005. Disappearing Arctic lakes. *Science* 308 (5727), 1429.
- Smith, L.C., Pavelsky, T.M., MacDonald, G.M., Shiklomanov, A.I., Lammers, R.B., 2007. Rising minimum daily flows in northern Eurasian rivers: a growing influence of groundwater in the high-latitude hydrologic cycle. *J. Geophys. Res. Biogeosci.* 112 (G4), G04S47.
- Smith, S.L., Romanovsky, V.E., Lewkowicz, A.G., Burn, C.R., Allard, M., Clow, G.D., Yoshikawa, K., Throop, J., 2010. Thermal state of permafrost in North America: a contribution to the international polar year. *Permafrost. Periglacial Process.* 21 (2), 117–135.
- Solomon, S., Qin, D., Manning, M., Chen, Z., Marquis, M., Averyt, K., Tignor, M., Miller, H. (Eds.), 2007. *Climate change 2007: the physical science basis. Contributions of Working Group I to the Fourth Assessment Report of the Intergovernmental Panel on Climate Change.* Cambridge University Press, Cambridge (1056 pp.).
- Spaans, E.J.A., Baker, J.M., 1996. The soil freezing characteristic: its measurement and similarity to the soil moisture characteristic. *Soil Sci. Soc. Am. J.* 60 (1), 13–19.
- St. Jacques, J., Sauchyn, D.J., 2009. Increasing winter baseflow and mean annual streamflow from possible permafrost thawing in the Northwest Territories, Canada. *Geophys. Res. Lett.* 36 (1), L01401.
- Stallman, R.W., 1963. Computation of ground-water velocity from temperature data. Methods of collecting and interpreting ground-water data. U.S. Geological Survey Water Supply Paper 1544-H. USGS, Reston, Virginia, pp. 35–46.
- Stallman, R.W., 1965. Steady one-dimensional fluid flow in a semi-infinite porous medium with sinusoidal surface temperature. *J. Geophys. Res.* 70 (12), 2821–2827.
- Stieglitz, M., Dery, S., Romanovsky, V., Osterkamp, T., 2003. The role of snow cover in the warming of Arctic permafrost. *Geophys. Res. Lett.* 30 (13), 1721.
- Streletskiy, D.A., Shiklomanov, N.I., Nelson, F.E., 2012. Spatial variability of permafrost active layer thickness under contemporary and projected climate in Northern Alaska. *Polar Geogr.* 35 (2), 95–116.
- Suzuki, S., 1960. Percolation measurements based on heat flow through soil with special reference to paddy fields. *J. Geophys. Res.* 65 (9), 2883–2885.
- Tan, X., Chen, W., Tian, H., Cao, J., 2011. Water flow and heat transport including ice/water phase change in porous media: numerical simulation and application. *Cold Reg. Sci. Technol.* 68 (1–2), 74–84.
- Taniguchi, M., Kayane, I., 1986. Changes in soil temperature caused by infiltration of snowmelt water. *Proceedings of IAHS Budapest Symposium.* pp. 93–101.
- Taniguchi, M., Shimada, J., Tanaka, T., Kayane, I., Sakura, Y., Shimano, Y., Dapaah-Siakwan, S., Kawashima, S., 1999a. Disturbances of temperature–depth profiles due to surface climate change and subsurface water flow: 1. An effect of linear increase in surface temperature caused by global warming and urbanization in the Tokyo Metropolitan Area, Japan. *Water Resour. Res.* 35 (5), 1507–1517.
- Taniguchi, M., Williamson, D.R., Peck, A.J., 1999b. Disturbances of temperature–depth profiles due to surface climate change and subsurface water flow: 2. An effect of step increase in surface temperature caused by forest clearing in southwest western Australia. *Water Resour. Res.* 35 (5), 1519–1529.
- Taniguchi, M., Shimada, J., Uemura, T., 2003. Transient effects of surface temperature and groundwater flow on subsurface temperature in Kumamoto Plain, Japan. *Phys. Chem. Earth, A/B/C* 28 (9–11), 477–486.
- Taniguchi, M., Burnett, W.C., Ness, G.D., 2008. Integrated research on subsurface environments in Asian urban areas. *Sci. Total Environ.* 404 (2–3), 377–392.
- Tao, Y., Gray, D.M., 1994. Prediction of snowmelt infiltration into frozen soils. *Heat Transf. A* 26 (2), 643–665.
- Tarnocai, C., Canadell, J.G., Schuur, E.A.G., Kuhry, P., Mazhitova, G., Zimov, S., 2009. Soil organic carbon pools in the northern circumpolar permafrost region. *Glob. Biogeochem. Cycles* 23, GB2023.
- Taylor, G.S., Luthin, J.N., 1978. A model for coupled heat and moisture transfer during soil freezing. *Can. Geotech. J.* 15 (4), 548–555.
- Taylor, C.A., Stefan, H.G., 2009. Shallow groundwater temperature response to climate change and urbanization. *J. Hydrol.* 375 (3–4), 601–612.
- Taylor, R.G., Scanlon, B., Döll, P., Rodell, M., van Beek, R., Wada, Y., Longuevergne, L., Leblanc, M., Famiglietti, J.S., Edmunds, M., Konikow, L., Green, T.R., Chen, J., Taniguchi, M., Bierkens, M.F.P., MacDonald, A., Fan, Y., Maxwell, R.M., Yecheili, Y., Gurdak, J.J., Allen, D.M., Shamsudduha, M., Hiscock, K., Yeh, P., Holman, I., Treidel, H., 2013. Ground water and climate change. *Nat. Clim. Chang.* 3, 322–329.
- Therrien, R., McLaren, R.G., Sudicky, E.A., Park, Y.J., 2012. *HydroGeoSphere: A Three-dimensional Numerical Model Describing Fully-integrated Subsurface and Surface Flow and Solute Transport Available at:* <http://hydrogeosphere.org/hydrosphere.pdf>.
- Tóth, J., 1963. A theoretical analysis of groundwater flow in small drainage basins. *J. Geophys. Res.* 68 (16), 4795–8812.
- Travis, B.J., Rosenberg, N.D., 1997. Modeling in situ bioremediation of TCE at Savannah River: effects of product toxicity and microbial interactions on TCE degradation. *Environ. Sci. Technol.* 31 (11), 3093–3102.
- Trefry, M.G., Muffels, C., 2007. FEFLOW: a finite-element ground water flow and transport modeling tool. *Ground Water* 45 (5), 525–528.
- Uchida, Y., Hayashi, T., 2005. Effects of hydrogeological and climate change on the subsurface thermal regime in the Sendai Plain. *Phys. Earth Planet. Inter.* 152 (4), 292–304.
- Uchida, Y., Sakura, Y., Taniguchi, M., 2003. Shallow subsurface thermal regimes in major plains in Japan with reference to recent surface warming. *Phys. Chem. Earth A/B/C* 28 (9–11), 457–466.
- Usowicz, B., 1995. Evaluation of methods for thermal conductivity calculations. *Int. Agrophys.* 9 (2), 109–113.
- Utting, N., Clark, I., Lauriol, B., Wieser, M., Aeschbach-Hertig, W., 2012. Origin and flow dynamics of perennial groundwater in continuous permafrost terrain using isotopes and noble gases: case study of the Fishing Branch River, Northern Yukon, Canada. *Permafrost. Periglacial Process.* 23 (2), 91–106.
- van der Gun, J., 2012. *Groundwater and global change: trends, opportunities and challenges.* World Water Assessment Programme Side Publications Series UNESCO, Paris, France (38 pp.).
- van der Kamp, G., Bachu, S., 1989. Use of dimensional analysis in the study of thermal effects of various hydrogeological regimes. *Hydrogeological regimes and their subsurface thermal effects.* Geophysical Monograph, 47. American Geophysical Union, Washington DC, pp. 23–28.
- Voss, C.I., 1984. A finite-element simulation model for saturated–unsaturated, fluid density-dependent ground-water flow with energy transport or chemically reactive single-species solute transport. U.S. Geological Survey Water-Resources Investigations USGS, Denver, CO (427 pp.).
- Voss, C.I., Provost, A.M., 2010. SUTRA: a model for saturated–unsaturated variable-density ground-water flow with solute or energy transport. U.S. Geological Survey Water-Resources Investigations U.S. Geological Survey, Reston, Virginia (260 pp.).
- Voytek, E.B., Drenkelfuss, A., Day-Lewis, F.D., Healy, R., Lane Jr., J.W., Werkema, D., 2014. 1DTempPro: analyzing temperature profiles for groundwater/surface-water exchange. *Ground Water* 52 (2), 298–302.
- Vyalov, S.S., Fortiev, S.M., Gerasimov, A.S., Zolotar, A.I., 1993. Provision for bearing capacity of permafrost soils in conditions of climate warming. *Soil Mech. Found. Eng.* 30 (6), 223–228.
- Walvoord, M.A., Striegl, R.G., 2007. Increased groundwater to stream discharge from permafrost thawing in the Yukon River basin: potential impacts on lateral export of carbon and nitrogen. *Geophys. Res. Lett.* 34 (12), 1–6.
- Walvoord, M.A., Voss, C.I., Wellman, T.P., 2012. Influence of permafrost distribution on groundwater flow in the context of climate-driven permafrost thaw: example from Yukon Flats Basin, Alaska, United States. *Water Resour. Res.* 48 (7), W07524.
- Watanabe, K., Kito, T., Wake, T., Sakai, M., 2011. Freezing experiments on unsaturated sand, loam and silt loam. *Ann. Glaciol.* 52 (58), 37–43.
- Wellman, T.C., Voss, C.I., Walvoord, M.A., 2013. Impacts of climate lake size, and supra- and sub-permafrost groundwater flow on Lake-Talik evolution, Yukon Flats, Alaska (USA). 21 (1), 281–298.
- Westermann, S., Boike, J., Langer, M., Schuler, T.V., Eitzelmlüller, B., 2011. Modeling the impact of wintertime rain events on the thermal regime of permafrost. *Cryosphere* 5 (4), 945–959.
- Wilby, R.L., Dawson, C.W., 2013. The statistical downscaling model: insights from one decade of application. *Int. J. Climatol.* 33 (7), 1707–1719.
- Williams, J.R., 1970. *Ground water in the permafrost regions of Alaska.* U.S. Geological Survey Professional Paper 696 U.S. Government Printing Office, Washington (83 pp.).
- Williams, P.J., Smith, M.W., 1989. *The Frozen Earth: Fundamentals of Geocryology.* Cambridge University Press, Cambridge; New York (306 pp.).
- Wisser, D., Marchenko, S., Talbot, J., Treat, C., Frolking, S., 2011. Soil temperature response to 21st century global warming: the role of and some implications for peat carbon in thawing permafrost soils in North America. *Earth Syst. Dyn.* 2 (1), 161–210.
- Woo, M., 1986. Permafrost hydrology in North America. *Atmosphere-Ocean* 24 (3), 201–234.
- Woo, M., 2012. *Permafrost Hydrology.* Springer-Verlag, Berlin (519 pp.).
- Woo, M., Kane, D.L., Carey, S.K., Yang, D., 2008. Progress in permafrost hydrology in the new millennium. *Permafrost. Periglacial Process.* 19 (2), 237–254.
- Wood, A.W., Leung, L.R., Sridhar, V., Lettenmaier, D.P., 2004. Hydrological implications of dynamical and statistical approaches to downscaling climate model outputs. *Clim. Chang.* 62 (1–3), 189–216.
- Woodbury, A.D., Smith, L., 1985. On the thermal effects of three-dimensional groundwater flow. *J. Geophys. Res.* 90 (2), 759–767.
- Wu, Q., Zhang, T., Liu, Y., 2012. Thermal state of the active layer and permafrost along the Qinghai–Xizang (Tibet) railway from 2006 to 2010. *Cryosphere* 6 (3), 607–612.
- Yang, M., Nelson, F.E., Shiklomanov, N.I., Guo, D., Wan, G., 2010. Permafrost degradation and its environmental effects on the Tibetan Plateau: a review of recent research. *Earth-Sci. Rev.* 103 (1–2), 31–44.
- Yoshikawa, K., Hinzmann, L., 2003. Shrinking thermokarst ponds and groundwater dynamics in discontinuous permafrost near Council, Alaska. *Permafrost. Periglacial Process.* 14 (2), 151–160.
- Zhang, T.J., 2005. Influence of the seasonal snow cover on the ground thermal regime: an overview. *Rev. Geophys.* 43 (4), RG4002.
- Zhang, Z., Wu, Q., 2012. Thermal hazards zonation and permafrost change over the Qinghai–Tibet Plateau. *Nat. Hazards* 61 (2), 403–423.
- Zhang, T., Barry, R., Gilichinsky, D., Bykhovets, S., Sorokovikov, V., Ye, J., 2001. An amplified signal of climatic change in soil temperatures during the last century at Irkutsk, Russia. *Clim. Chang.* 49 (1–2), 41–76.
- Zhang, Y., Chen, W.J., Cihlar, J., 2003. A process-based model for quantifying the impact of climate change on permafrost thermal regimes. *J. Geophys. Res. Atmos.* 108 (D22), 4695.
- Zhang, X., Sun, S., Xue, Y., 2007. Development and testing of a frozen soil parameterization for cold region studies. *J. Hydrometeorol.* 8 (4), 690–701.
- Zhang, Y., Carey, S.K., Quinton, W.L., 2008a. Evaluation of the algorithms and parameterizations for ground thawing and freezing simulation in permafrost regions. *J. Geophys. Res. Atmos.* 113 (17), D17116.
- Zhang, Y., Chen, W., Riseborough, D.W., 2008b. Transient projections of permafrost distribution in Canada during the 21st century under scenarios of climate change. *Glob. Planet. Chang.* 60 (3–4), 443–456.
- Zhao, L., Gray, D.M., Male, D.H., 1997. Numerical analysis of simultaneous heat and mass transfer during infiltration into frozen ground. *J. Hydrol.* 200 (1–4), 345–363.
- Zhu, K., Bayer, P., Grathwohl, P., Blum, P., 2014. Analysis of groundwater temperature evolution in the subsurface urban heat island of Cologne, Germany. *Hydrol. Process.* <http://dx.doi.org/10.1002/hyp.10209> (Published online).